DOCTORAL DISSERTATION

Effect of Entanglement between Cyclic and Linear Polymer on Crystallization under Quiescent and Flow Field

March 2023

Keiko Kobayashi

Graduate School of Environmental and Life Science

(Doctoral Course)

OKAYAMA UNIVERSITY

CONTENTS

Chapter 2

Role of entanglement species in the formation of shish-like fibril crystals elucidated by cyclic polyethylene

Chapter 3

Formation of shish-like fibril crystals from the melt of blends of cyclic and linear polyethylene under shear flow

General Introduction

Nowadays, a wide variety of polymers are commercially produced and available, and the demand for polymer materials with higher performance and functionality continues to grow. Additionally, the increasing production and consumption of polymer materials have a significant impact on the environment such as marine pollution, and this impact has become increasingly serious in recent years [1,2]. Therefore, it is necessary to reduce the environmental stress caused by polymer materials at a global level. To address these issues, it is essential to understand the molecular-level mechanisms of polymer structural formation and apply this knowledge to the development of new materials. This is expected to lead to the creation of multi-purpose polymer materials from only a few types of polymer species.

Since most polymers are semi-crystalline, understanding how polymer chains disentangle, rearrange, and diffuse to form crystals is crucial [3–6]. Controlling chain arrangements is one of the most important processes in polymer crystallization because it significantly affects the structural formation process of crystals and is crucial to the processing of polymer materials. The chain arrangements involve processes such as the disentanglement of polymer chains, orientation by flow, and diffusion within the melt or crystal.

The entanglement of polymer chains is a crucial factor in determining the arrangement of these chains. This is unique to polymers and occurs due to the long and flexible nature of their molecular chains. Polymer chains in a melt are known to exist in random coils that are entangled with one another. The "tube model" by de Gennes [7] and Doi and Edwards [8] is a commonly used abstract representation of entanglement, where the topological binding of a single molecular chain to the surrounding chains is depicted

as a hollow tube. The entanglement of polymer chains is resolved through the reptation of one chain in the direction of the chain axis through the hollow tube formed by other chains, as molecular chains cannot cross each other. It is important to note that the essence of entanglement lies in the intramolecular or intermolecular interaction that restricts the motion of molecular chains. From a macroscopic viewpoint, entanglement can be regarded as a phenomenon that constrains the movement of molecular chains, but from a microscopic viewpoint, the types of entanglement that can be formed differ in complexity, which can make them either difficult or easy to disentangle. This, in turn, can have varying effects on the structural formation process and its magnitude.

Uehara et al. conducted a series of studies on the disentangling behavior of entanglements during the melt-drawing process by *in-situ* pulse NMR measurements or wide and small angle X-ray scattering measurements of ultra-high molecular weight polyethylene [9–14]. They found that entanglements with varying ease of disentangling coexist and distinguished between "mobile" and "rigid" entanglements, which are easily disentangled and difficult to disentangle, respectively. The study also found that entanglements coexist in samples synthesized using Ziegler catalysts [15] with different molecular weight distributions and metallocene catalysts [15]. Samples synthesized with Ziegler catalysts were compared to those synthesized with metallocene catalysts, which have different molecular weight distributions.

Yamazaki et al [16]. investigated the entanglement of polymer chains by observing the nucleation process of polyethylene using a polarizing optical microscope. They clarified the time evolution of two-step entanglement from a polymer melt where no entanglement initially existed. They proposed different types of entanglements, including twists and knots, which are entanglements formed by twisting chains and entanglements

in which chains form knots at the ends. They observed that twists form earlier in the melt annealing time because they are easier to form than knots, and more complex entanglements form with increasing annealing time.

The molecular weight between entanglement points (M_e) of polyethylene chains is an important value when considering the entanglement of polymer chains, and it is a well-known value determined by rheological measurements [17]. However, entanglements that are easy to disentangle are considered difficult to measure by rheological measurements because they can be easily disentangled. Therefore, the M_e is considered inconsistent between the value obtained from a macroscopic point of view, such as rheological measurements, and the value obtained from a microscopic point of view through crystallization observations.

The M_e is unique to each polymer chain, and several methods have been used to estimate it, including melt rheological measurements, NMR relaxation measurements, and Monte Carlo simulations. There are many reports on the M_e value of polyethylene, but the values differ depending on the measurement methods used. For example, rheological measurements have reported a range of 830–2600 g/mol [18–25], NMR measurements have reported 1230 g/mol [26], and Monte Carlo simulations have reported 710–840 g/mol [27,28]. Litvinov et al. reexamined the M_e of polyethylene using NMR relaxation measurements and calculated a value of $M_e \approx 1760$ g/mol [29,30]. This value differs from the generally accepted $M_e \approx 1250$ g/mol determined from the plateau modulus but does not deviate from the range of values determined by rheological measurements.

Litvinov et al. have put forward the idea that the deviation in the value of M_e obtained from the generally accepted value may be since the effects of molecular weight distribution and branching were not properly evaluated during the measurement of

plateau modulus. This limitation may affect the validity of the hypotheses in the theory of rubber elasticity. Saalwächter responded to this report by Litvinov et al. and expressed his opinion that macro parameters from rheological measurements are often confused with micro parameters from NMR relaxation measurements. He also criticized the validity of the hypotheses used in the derivation process of the equations used in the analysis [31]. Therefore, it is considered that there is still much room for further study in the report of Litvinov et al.

However, it is significant to re-examine M_e, a fundamental parameter for entanglement, from a microscopic point of view through crystallization observations, as it may be possible to visualize various types of entanglement in polymers. The number of carbons required to form a single knot entanglement for the knot entanglements that linear polymers can form was simulated by de Gennes [32]. The knot entanglement assumed here is a "tight knot" entanglement, which is even more difficult to disentangle than usual. According to de Gennes, these tight knots can be formed by approximately 36–38 carbons, depending on the conformation of the trans and gauche, corresponding to a molecular weight of approximately 430–460 g/mol. Such entanglements are difficult to relax and eliminate in the melt.

The formation of tight knots with such characteristics occurs under limited conditions, and it is still unclear whether they form or not. However, the fact that the molecular weight of a flexible chain can be assumed to be such that the knot entanglement, which is difficult to disentangle, can be formed, is very important for the molecular interpretation of M_e. As described above, the entanglement of chains is crucial in the structure formation of polymers and has been extensively studied by many researchers. It is essential to study the various types of entanglement that can be formed from a molecular theoretical

viewpoint. Therefore, the M_e has been studied from a microscopic viewpoint through crystallization observation, and entanglement has been studied from a molecular theoretical viewpoint using simulations.

However, since entanglement can only be measured by observing the response or crystallization behavior of a solid or melt when an external stimulus is applied, the fact that the entanglement of molecular chains cannot be directly observed makes understanding entanglement more difficult. There are still many unknowns about entanglement that remain unclear.

Cyclic polymers are an interesting subject for investigating the role of entanglement species in polymer crystallization [33,34]. Because cyclic polymers lack chain ends, they cannot form knot entanglements and have fewer entanglements than linear polymers. This topological difference suggests that entanglements formed by cyclic polymers are easier to disentangle than those formed by linear polymers. Rheological studies of cyclic polymers were conducted by Roovers and McKenna et al. in the 1980s. Roovers et al. discovered [35,36] that the intermolecular diffusion of cyclic polymers is much slower than that of linear polymers, and they estimated that the entanglement density of cyclic polymers is approximately one-fifth of that of linear polymers with the same molecular weight. McKenna et al. also compared the zero-shear viscosity of cyclic and linear polystyrene of similar molecular weight during the same period as Roovers et al., finding that the zero-shear viscosity of cyclic polystyrene is about half that of linear polystyrene [37,38]. With advances in synthesis technology, experimental studies on the crystallization of cyclic polymers under quiescent conditions have become more prevalent. However, conflicting conclusions have been drawn from the comparison of the crystallization rates between cyclic and linear polymers, and further research is needed to

clarify this issue. Recently, a study on the crystallization of blended systems of cyclic and linear polymers under quiescent conditions was reported [34,39]. It is worth noting that there are almost no studies on the crystallization of cyclic polymers under the flow field, except for theoretical and simulation-based studies.

The entanglements also play a critical role in crystallization under the flow field [40,41]. In the flow field, polymer chains in the melt are elongated at the entanglement points, generating various morphologies such as core-skin, row nucleation, and shish-kebab structures. The formation mechanism of shish-kebab crystals, which consist of single fiber-like crystals called shish and folded chain crystals called kebab, has been discussed for a long time. Several models, such as the coil-stretch model proposed by de Gennes [42] and later examined by Keller et al. [43,44], have been verified. According to the widely accepted model, polymer chains elongated at the entanglements by the flow field form the oriented melt and grow to shish. After the formation of the shish, kebabs are epitaxially generated on the surface of the formed shish. Therefore, the entanglements in the flow field have both contributions to the enhancement of the formation of the oriented melt and the suppression of crystallization.

The purpose of this thesis is to clarify the effects of entanglement species and novel entanglements formed by mixing cyclic and linear polymers on crystallization under the quiescent and flow field.

In Chapter 1, the isothermal crystallization behavior of blends of cyclic and linear polyethylene in the quiescent state is described. The molecular weight of cyclic and linear polyethylene is fixed at one specimen and the blend ratios of cyclic and linear polyethylene are changed. The effect of the entanglement species formed by cyclic, linear polyethylene, and their blends on the crystallization is investigated. The novel

entanglements formed by cyclic and linear polyethylenes play a major role in the suppression of crystallization.

In Chapter 2, the formation of shish-like fibril crystals from the sheared melt of cyclic polyethylene and its blend with linear polyethylene is described. The effect of the degree of supercooling on the formation rate of the shish-like fibril crystals of cyclic polyethylene is compared to that of a linear polyethylene homopolymer. Additionally, the control of the density and species of entanglements using a blend of cyclic polyethylene and linear polyethylene is attempted. The crystallization behavior of the sheared melt in the blended samples is also examined.

In Chapter 3, the formation of shish-like fibril crystals from the sheared melt of blends of cyclic and linear polyethylene is described. The molecular weight and blend ratios of cyclic and linear polyethylene are varied to control the entanglement density, and the effects of the entanglement state on the formation of shish-like fibril crystals are investigated. The enhancement and suppression effects of blends of cyclic and linear polyethylene on shear-induced crystallization are discussed.

Overall, this thesis contributes to the understanding of the effects of entanglement species and novel entanglements formed by mixing cyclic and linear polymers on crystallization under different conditions.

References

[1] Salt R. Your plastic footprint: The facts about plastic pollution and what you can do to reduce your footprint. Firefly Books Ltd.: Richmond Hill; 2020.

[2] Bonanno G, Orlando-Bonaca M. Plastic pollution and marine conservation: Approaches to protect biodiversity and marine life. Academic Press: Amsterdam; 2022.

[3] Mandelkern L, Crystallization of polymers. Vol 1. Equilibrium concepts. Cambridge University Press: Cambridge; 1964.

[4] Mandelkern L, Crystallization of polymers. Vol 2. Kinetics and mechanisms. Cambridge University Press: Cambridge; 2004.

[5] Wunderlich B. Macromolecular physics. Vol 2. Crystal nucleation, growth, annealing. Academic Press: New York; 1976.

[6] Wunderlich B. Macromolecular physics. Vol 3. Crystal melting. Academic Press: New York; 1980.

[7] de Gennes P G, Scaling concepts in polymer physics. Cornell University Press: New York; 1979.

[8] Doi M, Edwards S F, The theory of polymer dynamics. Oxford University Press: Oxford; 1990.

[9] Kakiage M, Uehara H, Yamanobe T. Novel in situ NMR measurement system for evaluating molecular mobility during drawing from highly entangled polyethylene melts. Macromol Rapid Commun. 2008;29:1571–1576.

[10] Kato S, Tanaka H, Yamanobe T, Uehara H. In situ analysis of melt-drawing behavior of ultrahigh molecular weight polyethylene films with different molecular weights: Roles of entanglements on oriented crystallization. J Phys Chem B. 2015;119:5062–5070.

[11] Tanaka H, Saijo S, Kakiage M, Yamanobe T, Uehara H. In-situ analysis for melt-drawing behavior of ultra-high molecular weight polyethylene / normal molecular weight polyethylene blend films. Polymer. 2021;213:123213.

[12] Yoshizawa H, Takazawa A, Kakiage M, Yamanobe T, Hayashi N, Hiraoka M, Masunaga H, Aoyama K, Uehara H. Actuation mechanism of drawn polyethylene evaluated by structural change during cyclic stretching/shrinking. Sens Actuators A Phys.

2021;323:112634.

[13] Takazawa A, Kakiege M, Yamanobe T, Uehara H, Shimizu Y, Ohnishi T, Wakabayashi Y, Inatomi K, Abe S, Aoyama K. Effect of blending small amount of high-density polyethylene on molecular entanglements during melt-drawing of ultrahigh-molecular-weight polyethylene. Polymer. 2022;241:124528.

[14] Yoshizawa H, Takazawa A, Kakiage M, Yamanobe T, Hayashi N, Hiraoka M, Masunaga H, Aoyama K, Uehara h. In-situ X-ray analyses of structural change during drawing and shrinking of linear low-density polyethylene film. J Robotics Mechatron. 2022;34:310–315.

[15] Moore Jr E P, Polypropylene handbook, Hanser Gardner Publications: New York; 1996.

[16] Yamazaki S, Gu F, Watanabe K, Okada K, Toda A, Hikosaka M. Two-step formation of entanglement from disentangled polymer melt detected by using nucleation rate. Polymer. 2006;47:6422–6428.

[17] Wu S. Chain structure, phase morphology, and toughness relationships in polymers and blends. Polym Eng Sci. 1990;30:753–761.

[18] Aguilar M, Vega J F, Sanz E, Martínez-Salazar J. New aspects on the rheological behaviour of metallocene catalysed polyethylenes. Polymer. 2001;42:9713–9721.

[19] Saeda S, Yotsuyanagai J, Yamagachi K. The relation between melt flow properties and molecular weight of polyethylene. J Appl Polym Sci. 1971;15:277–292.

[20] Raju V R, Smith G G, Marin G, Knox J C, Graessley W W. Properties of amorphous and crystallizable hydrocarbon polymers. Melt rheology of fractions of linear polyethylene. J Polym SciPolym Phys. 1979;17:1183–1195.

[21] Raju V R, Rachapudy H, Graessley W W. Properties of amorphous and crystallizable

hydrocarbon polymers. IV. Melt rheology of linear and star-branched hydrogenated polybutadiene. J Polym Sci Polym Phys. 1979;17:1223–1235.

[22] Pearson D S, Fetters L J, Graessley W W, Ver Strate G, von Meerwall E. Viscosity and self-diffusion coefficient of hydrogenated polybutadiene. Macromolecules. 1994;27:711–719.

[23] Ferry J D. Viscoelastic properties of polymers. John Wiley & Sons, Inc.: New York; 1980.

[24] Fetters L J, Lohse D J, Richter D, Witten T A, Zirkel A. Connection between polymer molecular weight, density, chain dimensions, and melt viscoelastic properties. Macromolecules. 1994;27:4639–4647.

[25] Fetters L J, Lohse D J, Graessley W W. Chain dimensions and entanglement spacings in dense macromolecular systems. J Polym Sci Part B: Polym Phys. 1999;37:1023–1033.

[26] Ries M E, Brereton M G, Ward I M, Cail J I, Stepto R F T. Rescaling approach to molecular orientation for NMR and optical properties of polymer networks. Macromolecules. 2002;35:5665–5669.

[27] Foteinopoulou K, Karayiannis N C, Mavrantzas V G. Primitive path identification and entanglement statistics in polymer melts: Results from direct topological analysis on atomistic polyethylene models. Macromolecules. 2006;39:4207–4216.

[28] Ramos, J, Vega J F, Theodorou D N, Martinez-Salazar J. Entanglement relaxation time in polyethylene: simulation versus experimental data. Macromolecules. 2008;41:2959–2962.

[29] Litvinov V M, Ries M E, Baughman T W, Henke A, Matloka P P. Chain entanglements in polyethylene melts. Why is it studied again? Macromolecules. 2013;46:541–547.

[30] Litvinov V M, Ries M E, Baughman T W, Henke A, Matloka P P. Reply to “Comment on ‘Chain entanglements in polyethylene melts. Why is it studied again?’” Macromolecules. 2013;46:5094–5096.

[31] Saalwächter K. Comment on “Chain entanglements in polyethylene Melts. Why is it studied again?” Macromolecules. 2013;46:5090–5093.

[32] de Gennes P G. Tight knots. Macromolecules. 1984;17:703–704.

[33] Tezuka Y. Topological polymer chemistry: Progress of cyclic polymer in syntheses, properties and functions. World Scientific Publishing Co Inc.: Singapore; 2013.

[34] Pérez-Camargo R A. Mugica A. Zubitur M. Müller A J. Crystallization of cyclic Polymers. Adv Polym Sci. 2015;93–132.

[35] Roovers J. The melt properties of ring polystyrenes. Macromolecules. 1985;18:1359–1361.

[36] Roovers J. Viscoelastic properties of polybutadiene rings. Macromolecules. 1988;21:1517–1521.

[37] McKenna G B, Hostetter B J, Hadjichristidis N, Fetters L J, Plazek D J. A study of the linear viscoelastic properties of cyclic polystyrenes using creep and recovery measurements. Macromolecules. 1989;22:1834–1852.

[38] McKenna G B, Hadziioannou G, Lutz P, Hild G, Strazielle C, Straupe C, Rempp P, Kovacs A J. Dilute solution characterization of cyclic polystyrene molecules and their zero-shear viscosity in the melt. Macromolecules. 1987;20:498–512.

[39] López J V, Pérez-Camargo R A, Zhang B, Grayson S M, Müller A J. The influence of small amounts of linear polycaprolactone chains on the crystallization of cyclic analogue molecules. RSC Adv, 2016;53:48049–48063.

[40] Reiter G, Strobl G R. Progress in understanding of polymer crystallization. Springer:

Heidelberg; 2007.

[41] Cui K, Ma Z, Tian N, Su F, Liu D, Li L. Multiscale and multistep ordering of flow-induced nucleation of polymers. Chem Rev. 2018;118:1840–1886.

[42] de Gennes P G. Coil-stretch transition of dilute flexible polymers under ultrahigh velocity gradients. J Chem Phys. 1974;60:5030–5042.

[43] Keller A, Kolnaar H W H. Flow induced orientation and structure formation. In: Meijer H (ed) Processing of polymers. Wiley-VCH, Weinheim. 1997;18:189–268.

[44] Lieberwirth L, Loos J, Petermann J, Keller A. Observation of shish crystal growth into nondeformed melts. J Polym Sci Part B: Polym Phys. 2000;38:1183–1187.

Chapter 1

Effect of blend ratio of cyclic and linear polyethylene blends on isothermal crystallization in quiescent state

1-1 Introduction

The crystallization mechanism of linear polymers in a quiescent state has been studied for several decades. Numerous studies have been devoted to the clarification of the effect of molecular weight on crystallization, such as studies on the crystallization of polyolefins and polyesters from the isotropic melts, because it is known that the topological nature of chain molecules is explicitly dependent on their molecular weight. For example, Hoffman et al. [1–3] conducted a series of studies on the crystal growth of polyethylene. Okui et al. reported the primary nucleation and crystal growth of several polymers in the melt [4]. The role of chain entanglements in polymer crystallization is one of the most challenging problems. Psarski et al. [5] and Hikosaka et al. [6] independently reported that entanglements suppress the nucleation and growth of polymers. However, it remains unclear which type of entanglements, among knots, twists, or threads, more strongly affects polymer crystallization.

Cyclic polymers have long been of interest because, unlike linear polymers, they have the unique topological feature of having no chain ends. Many studies on the viscoelastic properties of cyclic polymers have been conducted. These indicate that cyclic polymers have fewer entanglements than linear polymers because of their lack of knot entanglements [7]. In the last few decades, studies on the crystallization of cyclic polymers have remarkably increased [8–12]. The reported results are controversial, and discussions are still ongoing [12]. Therefore, this chapter is not intended to reach a

universal conclusion about whether cyclic and linear polymers crystallize faster.

More recently, López et al. [13] and Ruiz et al. [14] analyzed the crystallization of blends of cyclic and linear polyesters. In these cases, it is expected that the novel entanglements formed between the cyclic and linear polymers, known as the threading effect [13,14], play an important role. The influence of linear contaminants has been pointed out several times in the rheological behaviors. For example, Kapnistos et al. found that the entanglements formed by blending cyclic and linear polystyrene were more difficult to disentangle than those formed with cyclic polystyrene solely through stress relaxation [15].

This work investigates the crystallization behavior of blended C-PE and L-PE samples in a quiescent state. The M_w of C-PE and L-PE was fixed for each specimen, and the blend ratios of C-PE and L-PE were changed. The half-crystallization time ($t_{1/2}$) was measured for a fixed degree of supercooling (ΔT), and not for the fixed crystallization temperature (T_c). The effect of the entanglement species formed by C-PE and L-PE and their blends on the crystallization are discussed.

1-2 Experimental

1-2-1 Sample preparation

All samples used in this chapter were synthesized in the author's laboratory using methods reported elsewhere [16–18]. The typical procedures are briefly described below and are summarized in **Scheme 1.1**. Cyclic polyoctenamer (C-PO), as a precursor of C-PE, was prepared by metathesis polymerization using *cis*-cyclooctene (COT) as the monomer and a cyclic Ru-alkylidene complex (modified Grubbs catalyst) was used as the catalyst. The method of preparing the modified Grubbs catalyst has been reported

previously [16–18]. To control the M_w of C-PO, metathesis polymerizations were performed at different temperatures and with different polymerization times and amounts of added catalyst. The chemical structure of C-PO was confirmed by ^{1}H NMR, ^{13}C NMR, and FT-IR spectroscopy. Evidence for a cyclic architecture of C-POs was provided by the absence of signals from the end groups in ^{1}H NMR spectroscopy. It should be noted that the undetectability of signals from the end groups is not warranted for the perfect cyclic purity of C-PO prepared above. In the literature [18], it has been shown that the presence of acyclic Ru-alkylidene complexes or impurities such as *cis*-cyclooctadiene may produce linear contaminants. In this chapter, the production of the modified Grubbs catalyst was carefully monitored to the best of the author's ability. Then, according to the method reported by Hahn [19], C-PEs by hydrogenation of the corresponding C-POs with tri-*n*-propylamine and *p*-toluenesulfonyl hydrazide were prepared. The M_w of the C-PEs was calculated assuming 100% hydrogenation of C-PO. The completion of hydrogenation was confirmed by the disappearance of the olefinic signals from the FT-IR spectra.

L-PE was prepared by the hydrogenation of linear PO (L-PO), which was prepared by the metathesis polymerization of COT using a second-generation Grubbs catalyst. The chemical structures of L-PO and L-PE were also examined by ^{1}H NMR and FT-IR spectroscopy. The M_w of the L-PEs was also calculated assuming 100% hydrogenation of L-PO. The M_w of C-PO and L-PO was evaluated using the relationship between the intrinsic viscosity [η] and M_w in tetrahydrofuran at 30 °C reported by Bielawski et al. [16]. The M_w values of C-PE and L-PE were 175×10^3 and 154×10^3 g/mol, respectively. The equilibrium melting temperatures (T_m^0) of C-PE and L-PE [20–23] were calculated assuming that the T_m^0 of C-PE is equal to that of perfect extended chain crystals of L-PE possessing half the M_w of C-PE. The T_m^0 values of C-PE and L-PE were 140.9 and

146.1 °C, respectively. For the T_m^0 of blended samples (T_m^0(C/L)), it was assumed an additive property given by

$$T_m^0(\mathrm{C/L}) = \left(1 - \frac{\phi_{\text{L-PE}}}{100}\right) \times T_m^0(\text{C-PE}) + \frac{\phi_{\text{L-PE}}}{100} \times T_m^0(\text{L-PE}) \quad (1.1)$$

where T_m^0(C-PE) and T_m^0(L-PE) are the T_m^0 values of the C-PE and L-PE homopolymers, respectively. Since the blend of C-PE and L-PE can be regarded as a perfectly miscible system, this treatment is accepted as a first-order approximation.

A blend of C-PE and L-PE was prepared as follows: C-PE and L-PE homopolymers were mixed with hot *o*-xylene. The solution was poured into excess methanol and the precipitate was recovered. The powder-blended samples were then dried in vacuo. The weight fraction of L-PE ($\Phi_{\text{L-PE}}$) in the blended samples was varied from 0 to 100 wt%.

1-2-2 Instruments and measurements

The isothermal crystallization behavior in the quiescent state was observed through polarizing optical microscopy (POM; Olympus, BX-53) conducted using a hot stage (Linkam LK-600M) and differential scanning calorimetry (DSC; PerkinElmer, DSC 8000) under a nitrogen stream (20 mL/min) to avoid sample degradation. The samples were sandwiched between two cover glasses for POM and placed in an Al pan for DSC analysis. The temperature and shear profiles are shown in **Figure 1.1**. All samples were melted at a rate of 30 °C/min and annealed at a temperature above T_m^0 (melt annealing temperature T_{max} = 160 °C) for 1 min to erase the previous thermal history. The samples were then cooled down to T_c at a rate of 30 °C/min. The range of ΔT was 25–28 K. The isothermal crystallization behavior was recorded through POM using a video camera (Victor KY-F1030). During isothermal crystallization, the heat flow was also measured as a function of crystallization time *t* using DSC.

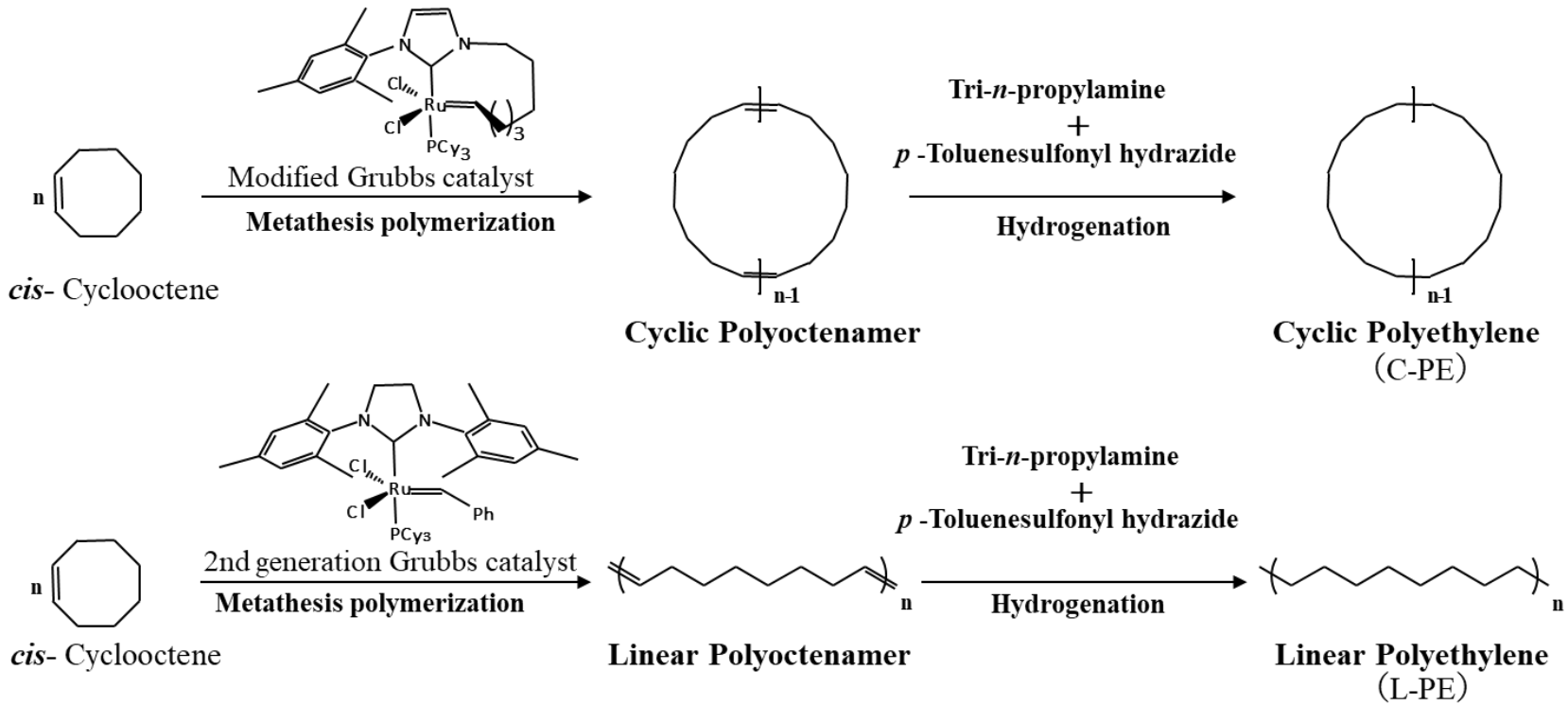

Scheme 1.1 Preparation of C-PE and L-PE.

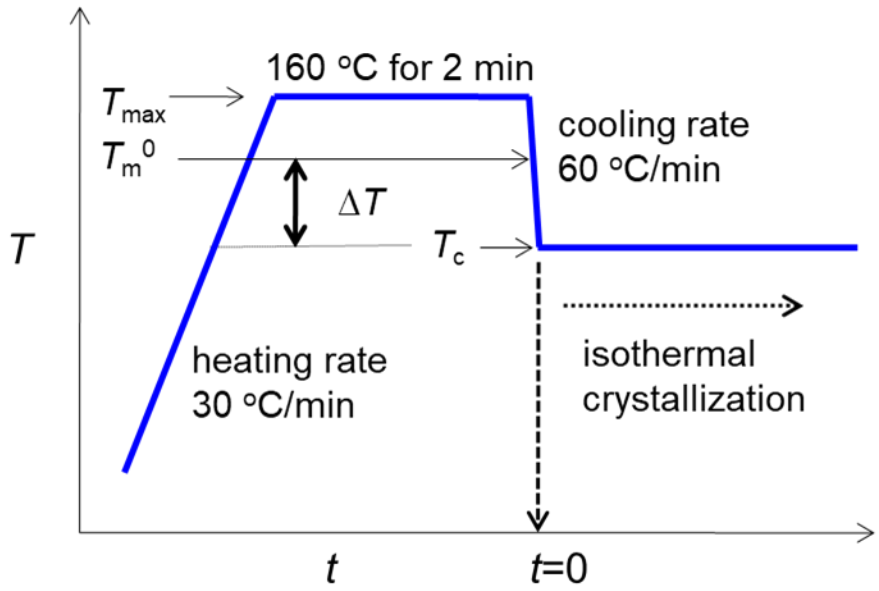

Figure 1.1 Melting and crystallization temperature, T, against crystallization time, t. All samples were melted and then kept at T_{max} (= 160 °C) for 2 min. After annealing, they were cooled to T_c to observe the crystallization.

1-2-3 Kinetic analysis with Avrami equation

In this chapter, the isothermal crystallization kinetics of the C-PE and L-PE blends were analyzed using the classical Avrami equation [23,24]. The Avrami equation can be expressed as:

$$1 - X_t = exp(-kt^n) \tag{1.2}$$

where X_t is the relative degree of crystallinity at crystallization time t, k is the overall crystallization rate constant, and n is the Avrami index. X_t can be defined as

$$X_t = \frac{\Delta H_t}{\Delta H_\infty} \tag{1.3}$$

where ΔH_t is the heat generated at t and ΔH_∞ is the total heat generated until the end of crystallization. Equation (1.2) can be transformed into a double logarithmic form as

follows:

$$\log[-\ln(1-\mathrm{X}_t)] = n\log t + \log k \tag{1.4}$$

The Avrami index n can be determined from the slope of the $\log[-\ln(1-\mathrm{X}_t)]$ vs. $\log t$ curve. The Avrami index n is related to the type of nucleation and geometry of the growing crystal, usually ranging from 0.5 to 4 [23]. By substituting $\mathrm{X}_t = 0.5$ into Equation (1.4), $t_{1/2}$, that is, the time necessary for the completion of 50% crystallization, can be obtained as:

$$t_{1/2} = (\ln 2/k)^{1/n} \tag{1.5}$$

It should be noted that the half-crystallization time includes the contribution of both primary nucleation and crystal growth. In this chapter, it is intended to prove the validity of the Avrami analysis, and it was only used for the quantitative estimation of $t_{1/2}$.

1-3 Results and discussion

1-3-1 Morphology of the blends of C-PE and L-PE observed by POM

Figure 1.2 shows typical examples of POM images of the crystals formed in the blends of C-PE and L-PE at (a) $\Phi_{\text{L-PE}}$ = 0 wt%, (b) $\Phi_{\text{L-PE}}$ = 50 wt%, and (c) $\Phi_{\text{L-PE}}$ = 100 wt%. ΔT and t were fixed at 26 K and 210 s, respectively. This crystallization period corresponds to the early stages of crystallization. It was found that the crystallization at $\Phi_{\text{L-PE}}$ = 0 wt%, that is, the C-PE homopolymer, was the fastest. The crystallization rate at $\Phi_{\text{L-PE}}$ = 100 wt%, that is, the L-PE homopolymer, was significantly slower than that of the C-PE homopolymer. Eventually, that at $\Phi_{\text{L-PE}}$ = 50 wt% was the slowest. The overall crystallization rate includes the contributions of both the primary nucleation rate and the crystal growth rate. Because the M_w of C-PE and L-PE are different, it is not easy to conclude which homopolymer has a faster crystallization rate. However, it seems to be

(a) $\Phi_{\text{L-PE}}$ = 0 wt%

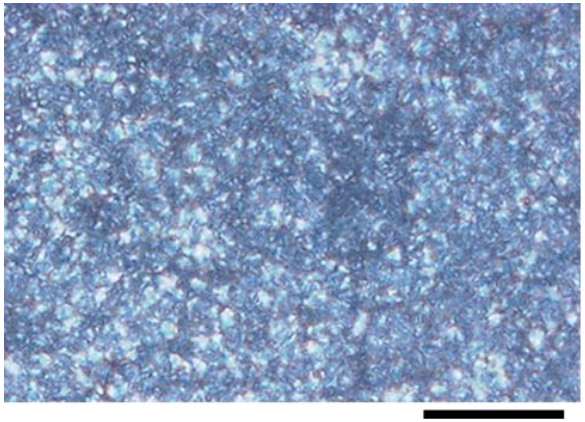

(b) $\Phi_{\text{L-PE}}$ = 50 wt%

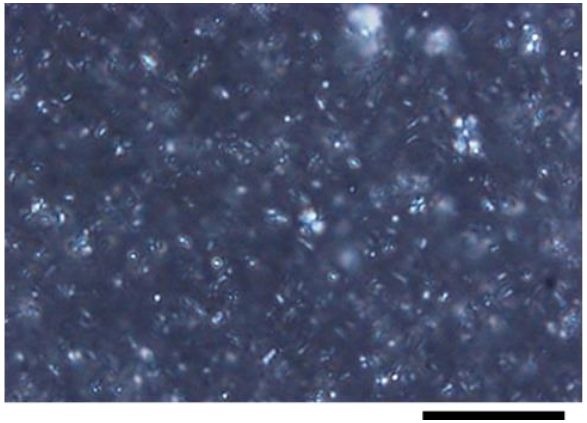

(c) $\Phi_{\text{L-PE}}$ = 100 wt%

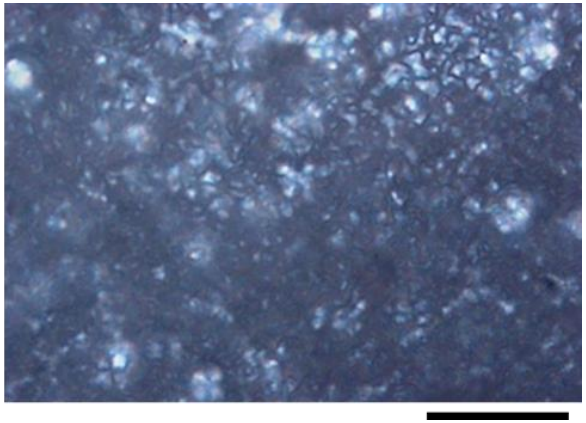

Figure 1.2 Typical examples of POM images of the formed crystals of the blends of C-PE and L-PE at (a) $\Phi_{\text{L-PE}}$ = 0 wt%, (b) $\Phi_{\text{L-PE}}$ = 50 wt%, and (c) $\Phi_{\text{L-PE}}$ = 100 wt%. ΔT and t were fixed at 26 K and 210 s. The scale bar represents 50 μm.

consistent with literature findings that the crystallization rate of cyclic polymers is higher than that of linear polymers, as reported by Su et al. [8], Pérez et al. [12], López et al. [13], and Ruiz et al. [14]. The morphology of the formed crystal does not seem to be significantly different irrespective of the blend ratio, as reported for cyclic and linear blends of poly(ε-caprolactone) [13] and poly(*L*-lactide) [14].

1-3-2 Crystallization kinetics of the blends of C-PE and L-PE

Figure 1.3 (a) shows a typical example of the time evolution of the heat flow for the blends of C-PE and L-PE at ΔT = 26 K. All samples show a uniform exothermic peak, although the half-widths of the peaks differ depending on the blend ratio. The peak positions of the C-PE and L-PE homopolymer, that is, $\Phi_{\text{L-PE}}$ = 0 and 100 wt%, were almost coincident. The peak position for $\Phi_{\text{L-PE}}$ = 50 wt% shifted to the slowest crystallization time. According to Equation (1.3), the time evolution of the heat flow was converted to that of the relative degree of crystallinity. **Figure 1.3** (b) shows a typical example of the time evolution of the relative degree of crystallinity X_t of the blends of C-PE and L-PE at ΔT = 26 K. All samples show a single sigmoidal curve irrespective of $\Phi_{\text{L-PE}}$. Compared with the data for $\Phi_{\text{L-PE}}$ = 0 and 100 wt%, the completion of crystallization for the former was faster than that for the latter. The onset and completion of crystallization at $\Phi_{\text{L-PE}}$ = 50 wt% were the slowest among all samples. **Figure 1.3** (c) shows a typical example of Avrami plots for the blends of C-PE and L-PE at $\Phi_{\text{L-PE}}$ = 0, 50, and 100 wt% at ΔT = 26 K. From the initial slope of the Avrami plots, the Avrami index *n* can be obtained. The obtained index *n* ranged from 1.5 to 2.2 and did not show a clear ΔT and $\Phi_{\text{L-PE}}$ dependence. Similar *n* values were reported by Krumme et al. for high-density polyethylene with high and low M_w [25].

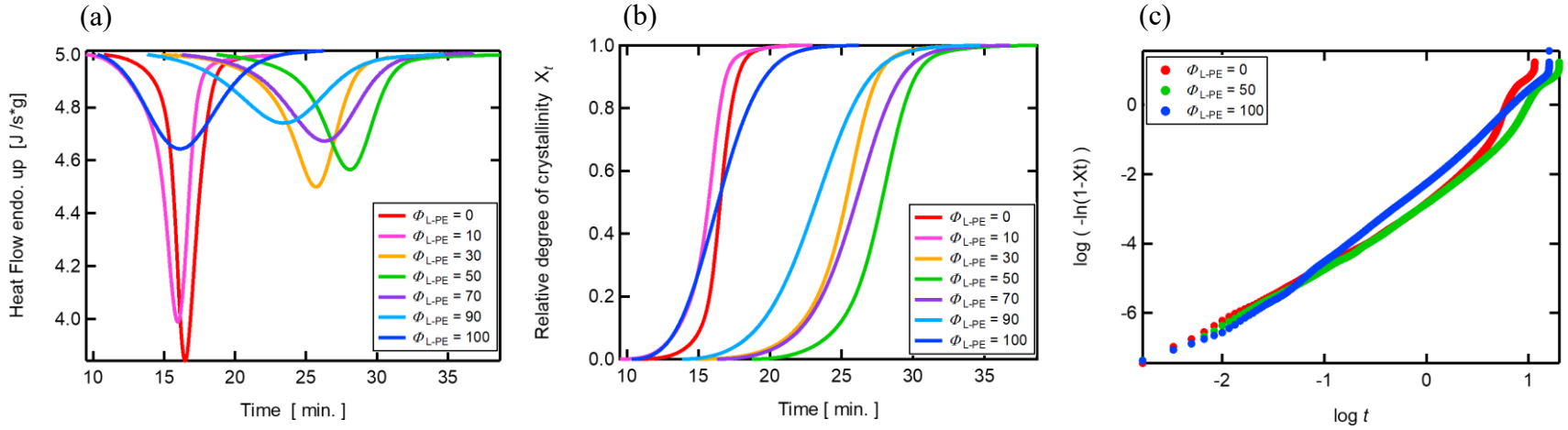

Figure 1.3 Typical example of the time evolution of (a) heat flow of the blends of C-PE and L-PE at ΔT = 26 K and(b) relative degree of crystallinity X_t of the blends of C-PE and L-PE at ΔT = 26 K. (c) Typical example of Avrami plots of the blends of C-PE and L-PE at $\Phi_{\text{L-PE}}$ = 0, 50, and 100 wt% at ΔT = 26 K.

Figure 1.4 shows plots of the inverse of the half-crystallization time ($1/t_{1/2}$) against $\Phi_{\text{L-PE}}$ for different ΔT. It was found that the $1/t_{1/2}$ for C-PE was almost the same as that for L-PE at ΔT = 27 K. At a lower ΔT, the former was significantly larger than the latter, and vice versa at a larger ΔT. As mentioned before, $t_{1/2}$ involves contributions from both primary nucleation and crystal growth. It is well known that primary nucleation density easily fluctuates depending on the density of heterogeneity within the system [6]. Compared to large ΔT where the contribution of nucleation is relatively low, it seems that C-PE crystalizes faster than L-PE. On the other hand, a minimum of $1/t_{1/2}$ was observed at approximately $\Phi_{\text{L-PE}}$ = 50 wt% irrespective of ΔT. López et al. [13] and Ruiz et al. [14] reported the plots of the inverse of the half-crystallization ($1/t_{1/2}$) against the weight fraction Φ of the cyclic polymer at a fixed T_c. They demonstrated a complicated Φ dependence on $1/t_{1/2}$. The difference between their results and this study may arise from the difference between plotting against T_c or ΔT. Further investigation is needed. Since crystallization is suppressed by the entanglements, the suppression effect of crystallization by the entanglements was maximized at $\Phi_{\text{L-PE}}$ = 50 wt%. The suppression effect should consider the contribution of both the quantity and disentangling ability. As reported by Roovers [7], the entanglement quantity, i.e., the number density of the entanglement (ν_e) of linear polymers is much larger than that of cyclic polymers with the same M_w. In this chapter, it was expected that L-PE would have a larger ν_e than C-PE because of the small difference in M_w between them. However, cyclic polymers have entanglements that are easy to disentangle owing to the lack of chain ends. The entanglements of linear polymers are more complicated and difficult to disentangle than those of cyclic polymers. Because the effects of ν_e and the disentangling ability on crystallization are offset, no influence of $1/t_{1/2}$ on the C-PE and L-PE homopolymers was

shown. In the blend of C-PE and L-PE, in addition to the entanglements formed by single polymers, the formation of a novel entanglement, such that the L-PE chain penetrates the C-PE ring, is expected. It is speculated that this type of entanglement is difficult to disentangle, as discussed by Ruiz et al. [14]. **Figure 1.5** shows a schematic illustration of the role of entanglement species in the crystallization of C-PE, L-PE, and their blends. Because the L-PE chains in the molten state are complexly entangled with each other, disentangling and chain diffusion become slower. Therefore, crystallization from such melts becomes slower. On the other hand, since C-PE chains can disentangle much easier, crystallization from such melts becomes faster. In the blends of C-PE and L-PE, owing to the novel complicated entanglement, the chains in the melt are difficult to be disentangled. Consequently, the crystallization of the blends was slower than that of the C-PE and L-PE homopolymers. it was speculated that this effect would be maximized at $\Phi_{\text{L-PE}}$ = 50 wt% when the M_w values of C-PE and L-PE in the blends were almost the same.

1-4 Conclusion

To clarify the effects of entanglement species on crystallization in a quiescent state, the $t_{1/2}$ of blends of C-PE and L-PE from the melt was studied as a function of $\Phi_{\text{L-PE}}$ and ΔT through POM and DSC. C-PE and L-PE were prepared with M_w of 175×10^3 and 154×10^3, respectively. The $1/t_{1/2}$ values of the C-PE and L-PE homopolymers are almost the same at ΔT = 27 K, with the former being slightly lower than the latter at a lower ΔT. In contrast, the $1/t_{1/2}$ values of the blends of C-PE and L-PE were significantly lower than those of the C-PE and L-PE homopolymers, and a minimum of $1/t_{1/2}$ was observed at $\Phi_{\text{L-PE}} \approx 50$ wt%. This suggests that the suppression of crystallization in the blended system was caused by a novel entanglement formed by the penetration of the L-PE chain into the

C-PE chain.

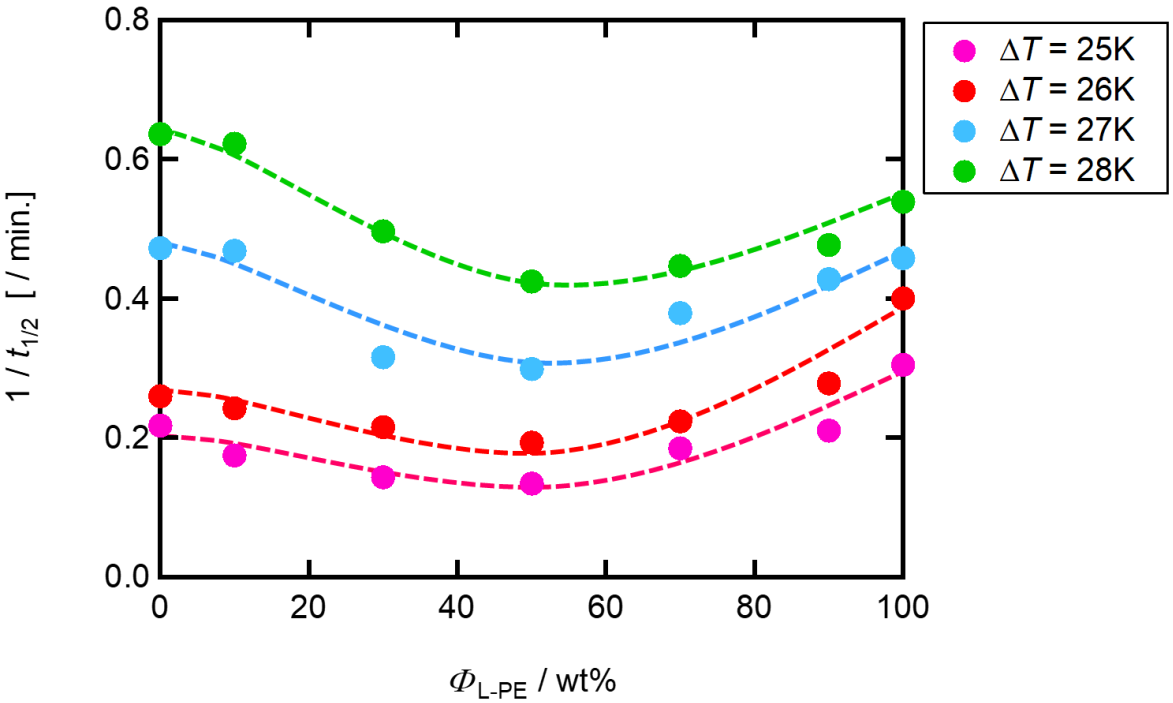

Figure 1.4 Plots of $1/t_{1/2}$ against $\Phi_{L\text{-}PE}$ for different ΔT.

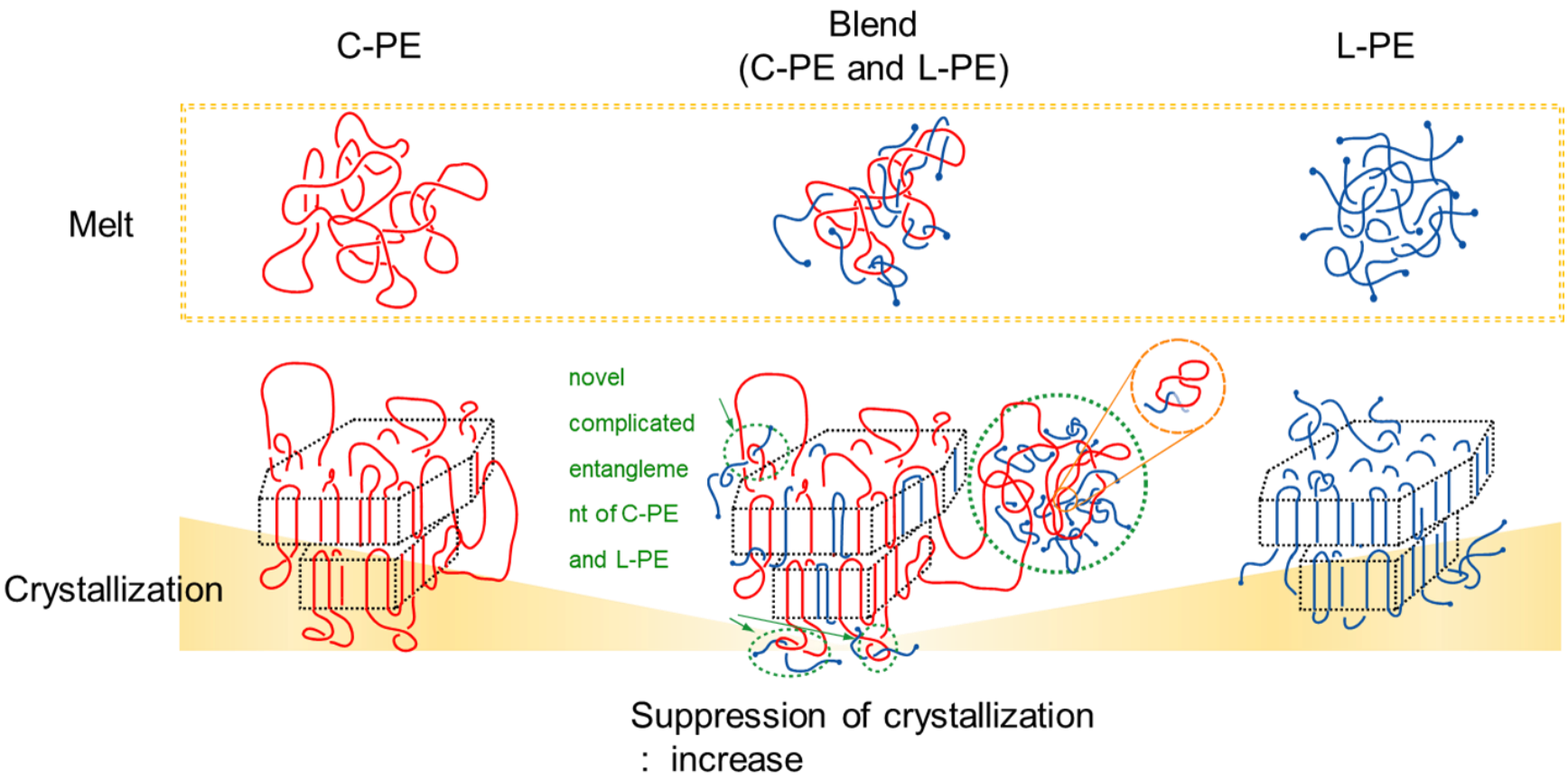

Figure 1.5 Schematic illustration of the role of entanglement species in the crystallization of C-PE and L-PE and their blends.

1-5 References

[1] Hoffman J D, Lauritzen J I. Crystallization of bulk polymers with chain folding: theory of growth of lamellar spherulites. J Res Natl Bur Stand A. 1961;65A:297–336.

[2] Hoffman J D, Lauritzen J I, Passaglia E, Ross G S, Frolen L J, Weeks J J. Kinetics of polymer crystallization from solution and the melt. Kolloid Z Z Polym. 1969;231:564–592.

[3] Hoffman J D, Frolen L J, Ross G S, Lauritzen J I. On the growth rate of spherulites and axialites from the melt in polyethylene fractions: Regime I and regime II crystallization. J Res Natl Bur Stand A. 1975;79A:671–679.

[4] Umemoto S, Okui N. Power law and scaling for molecular weight dependence of crystal growth rate in polymeric materials. Polymer. 2005;46:8790–8795.

[5] Psarski M, Piorkowska E, Galeski A. Crystallization of polyethylene from melt with lowered chain entanglements. Macromolecules. 2000;33:916–932.

[6] Hikosaka M, Watanabe K, Okada K, Yamazaki S. Topological mechanism of polymer nucleation and growth - The role of chain sliding diffusion and entanglement. Adv Polym Sci. 2005;191:137–186.

[7] Roovers J. Viscoelastic properties of polybutadiene rings. Macromolecules. 1988;21:1517–1521.

[8] Su H H, Chen H L, Díaz A, Casas M T, Puiggalí J, Hoskins J N, Grayson S M, Pérez R A, Müller A J. New insights on the crystallization and melting of cyclic PCL chains on the basis of a modified Thomson-Gibbs equation. Polymer. 2013;54:846–859.

[9] Tezuka Y, Ohtsuka T, Adachi K, Komiya R, Ohno N, Okui N. A Defect-free ring polymer: Size-controlled cyclic poly(tetrahydrofuran) consisting exclusively of the monomer unit. Macromol Rapid Commun. 2008;29:1237–1241.

[10] Takeshita H, Poovarodom M, Kiya T, Arai F, Takenaka K, Miya M, Shiomi T. Crystallization behavior and chain folding manner of cyclic, star and linear poly(tetrahydrofuran)s. Polymer. 2012;53:5375–5384.

[11] Ono R, Atarashi H, Yamazaki S, Kimura K. Molecular weight dependence of the growth rate of spherulite of cyclic poly(ε-caprolactone) polymerized by ring expansion reaction. Polymer. 2020;194:122403.

[12] Pérez R A, Córdova M E, López J V, Hoskins J N, Zhang B, Grayson S M, Müller A J. Nucleation, crystallization, self-nucleation and thermal fractionation of cyclic and linear poly(ε-caprolactone)s. React Funct Polym. 2014;80:71–82.

[13] López J V, Pérez-Camargo R A, Zhang B, Grayson S M, Müller A J. The influence of small amounts of linear polycaprolactone chains on the crystallization of cyclic analogue molecules. RSC Adv. 2016;6:48049–48063.

[14] Ruiz M B, Pérez-Camargo R A, López J V, Penott-Chang E, Múgica A, Coulembier O, Müller A J. Accelerating the crystallization kinetics of linear polylactides by adding cyclic poly (*L*-lactide): Nucleation, plasticization and topological effects. Int J Biol Macromol. 2021;186:255–267.

[15] Kapnistos M, Lang M, Vlassopoulos D, Pyckhout-Hintzen W, Richter D, Cho D, Chang T, Rubinstein M. Unexpected power-law stress relaxation of entangled ring polymers. Nat Mater. 2008;7:997–1002.

[16] Bielawski C W, Benitez D, Grubbs R H. An “Endless” route to cyclic polymers. Science. 2002;297:2041–2044.

[17] Fürstner A, Ackermann L, Gabor B, Goddard R, Lehmann C W, Mynott R, Stelzer F, Thiel O R. Comparative investigation of ruthenium-based metathesis catalysts bearing *N*-heterocyclic carbene (NHC) ligands. Chem Eur J. 2001;7:3236–3253.

[18] Bielawski, C W, Benitez D, Grubbs R H. Synthesis of cyclic polybutadiene via ring-opening metathesis polymerization: The importance of removing trace linear contaminants. J Am Chem Soc. 2003;125:8424–8425.

[19] Hahn S F. An improved method for the diimide hydrogenation of butadiene and isoprene containing polymers. J Polym Sci, Part A: Polym Chem. 1992;30:397–407.

[20] Wunderlich B, Czornyj G. A study of equilibrium melting of polyethylene. Macromolecules. 1977;10:906–913.

[21] Broadhurst M G. Extrapolation of the orthorhombic n-paraffin melting properties to very long chain lengths. J Chem Phys. 1962;36:2578–81.

[22] Broadhurst M G. The Melting Temperatures of the *n*-paraffins and the convergence temperature for polyethylene. J Res Natl Bur Stand A. 1966;70:481–486.

[23] Mandelkern L. Crystallization of polymers. Vol 2. Kinetics and mechanisms. Cambridge University Press: Cambridge; 2004.

[24] Lorenzo A T, Arnal M L, Albuerne J, Müller A J. DSC isothermal polymer crystallization kinetics measurements and the use of the Avrami equation to fit the data: Guidelines to avoid common problems. Polymer Testing, 2007;26:222–231.

[25] Krumme A, Lehtinen A, Viikna A. Crystallisation behaviour of high density polyethylene blends with bimodal molar mass distribution 1. Basic characteristics and isothermal crystallisation. Eur Polym J. 2004;40:359–369.

Chapter 2

Role of entanglement species in the formation of shish-like fibril crystals elucidated by cyclic polyethylene

2-1 Introduction

It is well known that shish-kebab crystals, which consist of an extended chain fibrillar core (shish) surrounded by folded chain lamellar crystals (kebab) attached to the shish, can form when linear polyolefins, such as polyethylene or polypropylene, are crystallized under external flow fields, such as shear and elongational flow [1–5]. Several possible mechanisms of shish formation have been reported [6–8], with the following scenario being one of the most promising. Random coiled chains within the melt are partially stretched by flow at the entanglement points, and an oriented melt is formed. The stretched chains are nucleated, and the bundle nuclei are grown to the shish. The kebabs are then epitaxially generated on the shish surface. According to this formation mechanism, entanglement is important for the formation of the shish [9–14], that is, the formation of the oriented melt, because the entanglements effectively function as a "topological pin" during chain stretching. It is natural to consider that the topological pinning effect increases in complicated entanglements, such as tight knots, rather than twisted entanglements [15–18]. The more complicated entanglements increase, the stronger the chain-stretching without chain disentanglement.

Using cyclic polymers, it is possible to control the entanglement species as they cannot form knot entanglements accompanied by chain ends. This implies that cyclic polymers have fewer entanglements than the linear analogs reported by Roovers [19]. Therefore, cyclic polymers are among the most suitable candidates for clarifying the

effect of entanglement species on shish formation. To the best of the author's knowledge, there have been no experimental studies on the shear-induced crystallization of cyclic polymers; however, there have been a few theoretical studies [20].

In this chapter, the shear-induced crystallization of a cyclic polyethylene (C-PE) homopolymer and its blend with linear polyethylene (L-PE) was investigated. The effect of the degree of supercooling (ΔT) on the formation rate (I) of the shish-like fibril crystals of C-PE was compared to that of L-PE homopolymer. Additionally, control of the density and species of entanglements using a blend of C-PE and L-PE was attempted. The crystallization behavior of the sheared melt in the blended samples was also examined.

2-2 Experimental

2-2-1 Sample preparation

The C-PE and L-PE used in this chapter were prepared using the same method reported elsewhere [21–23]. First, PE precursors such as cyclic and linear polyoctenamers were synthesized via the ring-opening metathesis polymerization of *cis*-cyclooctene catalyzed by **1** and **2**, respectively. Both PE precursors were hydrogenated with *p*-toluenesulfonyl hydrazide and converted to the corresponding PE. The chemical structures of all samples were confirmed by FT-IR (JASCO FT/IR-410 spectrometer), ^{1}H NMR and ^{13}C NMR (JEOL AL300 SC-NMR). The weight average molecular weights, M_w, of C-PE and L-PE were determined using the method described in Chapter 1 [21]. The M_w of the C-PE and L-PE precursors was converted to that of C-PE and L-PE assuming 100% hydrogenation. All samples were formed as a film by melt pressing for crystallization experiments.

The M_w, equilibrium melting temperature, T_m^0, and crystallization temperature, T_c

values of the C-PE and L-PE used in this chapter are summarized in **Table 2.1**. The T_m^0 of C-PE and L-PE [24–26] were calculated assuming that the T_m^0 of C-PE is equal to that of perfect extended chain crystals of L-PE possessing half the M_w of C-PE.

Small amounts of L-PE to C-PE were added to C-PE as follows. The C-PE and L-PE homopolymers were mixed in hot *o*-xylene. The solution was poured into excess methanol, and the precipitate was recovered. The powder-blended samples were dried in vacuo. The weight fraction of L-PE, $\Phi_{L\text{-}PE}$, in the blended sample was fixed at 1 and 3 wt%. Because the critical concentration for overlapping in bulk is calculated to be approximately 3 wt% [13,27], $\Phi_{L\text{-}PE}$ was set below this concentration.

Table 2.1 M_w, T_m^0, and T_c of C-PE and L-PE.

Code	M_w / g mol^{-1}	T_m^0 / °C	T_c / °C
C-PE(44k)	44×10^3	139.4	108.0–109.0
C-PE(115k)	115×10^3	140.5	111.0–113.5
L-PE(65k)	65×10^3	145.6	119.5–121.5
C-PE(44k) + L-PE(65k)	–	–	117.5–119.0

2-2-2 Instruments and measurements

The crystallization behavior of the sheared melt was observed using a polarizing optical microscope (POM; Olympus, BX-51) equipped with a hot stage (Linkam CSS-450). The hot stage consists of parallel plates made of quartz, with a gap between both plates (h) of 100 μm. The temperature and shear profiles are shown in **Figure 2.1**. All samples were melted at a rate of 30 °C/min and annealed at a temperature above T_m^0 (melt

annealing temperature, T_{max} = 150 °C) for 1 min. Then, the samples were cooled down to the desired T_c at a rate of 30 °C/min. Pulse shear flow was applied to the samples immediately before reaching T_c. The shear rate ($\dot{\gamma}$) and duration time of shear flow (τ_d) were fixed at 50 s^{-1} and 1 s, respectively. The ranges of ΔT were 26.5–31.4 K for C-PE and 24.1–26.1 K for L-PE. During isothermal crystallization, the number density of shish-like fibril crystals, i.e., the number density of the nuclei that grew to shish-like fibril crystals (N) was measured using a video camera (Victor KY-F550). The saturated value of N (ν_{st}) against the crystallization time t [23] was also measured. The formation rate of shish-like fibril crystals (I) was calculated by $I = dN/dt$ as a function of ΔT or T_c. As reported in a paper [11], N corresponds to the number of the nuclei.

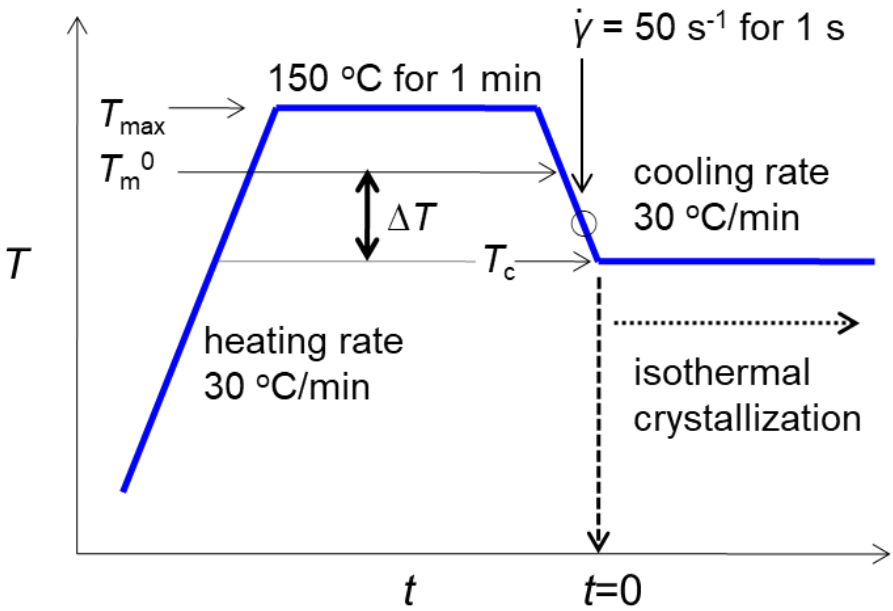

Figure 2.1 Melting and crystallization temperature, T, against crystallization time, t. All samples were melted and then kept at T_{max} (= 150 °C) for 1 min. After annealing, they were cooled to T_c to observe the crystallization. Pulsed shear flow with $\dot{\gamma}$ = 5 s^{-1} was applied immediately before reaching T_c.

To characterize the morphology of the shish-like fibril crystals, scanning electron microscopy (SEM) was performed using Hitachi S-2150. In the SEM observations, shish-like fibril crystals were initially prepared using the hot stage. The sample film, including shish-like fibril crystals in the molten state, was quenched to 20 °C. Then, shish-like fibril crystals within the sample were isolated from the sample film using the difference in melting temperature between shish-like fibril crystals and unoriented small crystals. Isolated shish-like fibril crystals were subjected to surface etching using decalin.

2-3 Results and discussion

2-3-1 Morphology of the shish-like fibril crystals of C-PE

Figure 2.2 (a) shows a POM image of the formation of shish-like fibril crystals of C-PE from the sheared melt at T_c = 113.5 °C. A similar morphology of fibril crystals has been observed for linear PE [11,12,27–29]. **Figure 2.2** (b) shows an SEM image of several strands of shish-like fibril crystals of C-PE extracted from a thin-film sample immediately after isothermal crystallization from the sheared melt. The fibril crystals within the sample can be observed as bundle-like structures, and the fiber axis coincided with the flow direction. The diameter d of a single strand of the shish-like fibril crystal was ~1.5 μm. To observe the inner morphology of shish-like fibril crystals in detail, rough etching of macroscopic strands of shish-like fibril crystals was conducted using decalin as a solvent. **Figure 2.2** (c) shows an SEM image of several etched strands of the shish-like fibril crystals. A macroscopic single strand was found to consist of a bundle of several microfibers with d = 1 μm. Because the extraction from the bulk sample was rough and incomplete, the inner structure of the microfiber was unknown. However, this does not imply that the microfiber is composed of a single extended chain crystal.

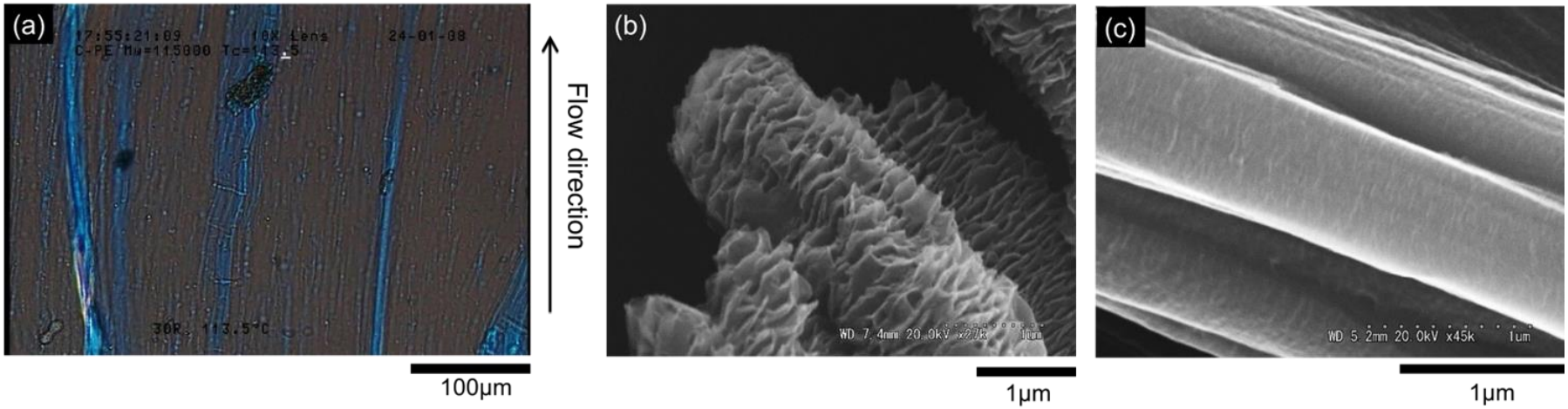

Figure 2.2 Morphology of (a) shish-like fibril crystals formed from the sheared melt observed by POM, (b) several strands of the shish-like fibril crystal, and (c) inner structure of several etched strands of the shish-like fibril crystal observed by SEM.

The T_m (nominal melting temperature) values of the observed shish-like fibril crystals and spherulites of C-PE and L-PE were also measured (**Table 2.2**). In both samples, the T_m of the shish-like fibril crystals was much higher than that of the spherulites. The Gibbs-Thomson equation [30] is expressed as

$$T_m = T_m^0 - \frac{c}{l} \tag{2.1}$$

where c and l are a constant and crystal thickness, respectively. From this equation, it is clear that the value of l for fibril crystals is much larger than that for spherulites. Therefore, it is considered that the observed fibril crystals correspond to overgrown assemblies of shish crystals generated from the elongated chains. Moreover, the T_m of the observed fibril crystals of C-PE was significantly lower than that of L-PE. The C-PE fibril crystals are somewhat unstable compared to the L-PE fibril crystals due to the topological constraint of C-PE being unable to elongate completely, that is, due to the existence of two permanent foldings in the fully stretched state. However, the morphologies of the fibril crystals of C-PE and L-PE were essentially identical. From these experimental findings, it is concluded that the fibril crystals of C-PE observed in this chapter can be regarded as assemblies of shish crystals [11,12,23,29,31].

Table 2.2 T_m of the observed fibril crystals and spherulites of C-PE and L-PE.

	T_m / °C	
Code	Shish-like fibril crystal	Spherulite
C-PE(115k)	136.8	129.6
L-PE(65k)	143.3	130.8

2-3-2 Comparison of *I* between C-PE and L-PE

Figure 2.3 shows plots of I against ΔT^{-2} for C-PE(115k) and L-PE(65k). It was found that I obeyed the well-known equation [32]

$$I = I_0\exp(-\Delta G^*/kT) = I_0\exp(-C/\Delta T^2) \tag{2.2}$$

where ΔG^* is the free energy required to form a critical primary nucleus and k is the Boltzmann constant. Therefore, the formation of shish-like fibril crystals of C-PE and L-PE can be regarded as a nucleation-controlled process. Although the slopes of the straight lines C were somewhat different, but not extremely changed, irrespective of the topological nature of the polymers.

According to classical nucleation theory [33], C is defined by

$$C \propto \sigma^2\sigma_e \tag{2.3}$$

where σ and σ_e are the side- and end-surface free energies of the nucleus, respectively. Although it is necessary for a few assumptions, it can be judged the type of nucleus, such as a fold or bundle nucleus, from the value of C. As reported by Yamazaki et al. [11], the type of nucleus of the L-PE shish was shown to be a bundle nucleus, and the value of C for the fold nucleus was much greater than that for the bundle nucleus. Therefore, it can be concluded that the nucleus of the shish-like fibril crystal of C-PE is also a bundled nucleus.

By contrast, considering that the values of M_w for C-PE(115k) and L-PE(65k) are different, a direct comparison of the values of the intercepts, I_0, for C-PE and L-PE must be made. The M_w of C-PE is approximately twice that of L-PE. When the molecules of C-PE(115k) and L-PE(65k) are fully stretched, the end-to-end lengths are approximately the same, and both C-PE(115k) and L-PE(65k) have comparable chain dimensions. In general, in primary nucleation, it was found that the value of I_0 should decrease with

increasing M_w [34,35]. This chapter reveals that the I_0 of C-PE(115k) was significantly smaller than that of L-PE(65k) by one order of magnitude, indicating that the former is more difficult to nucleate.

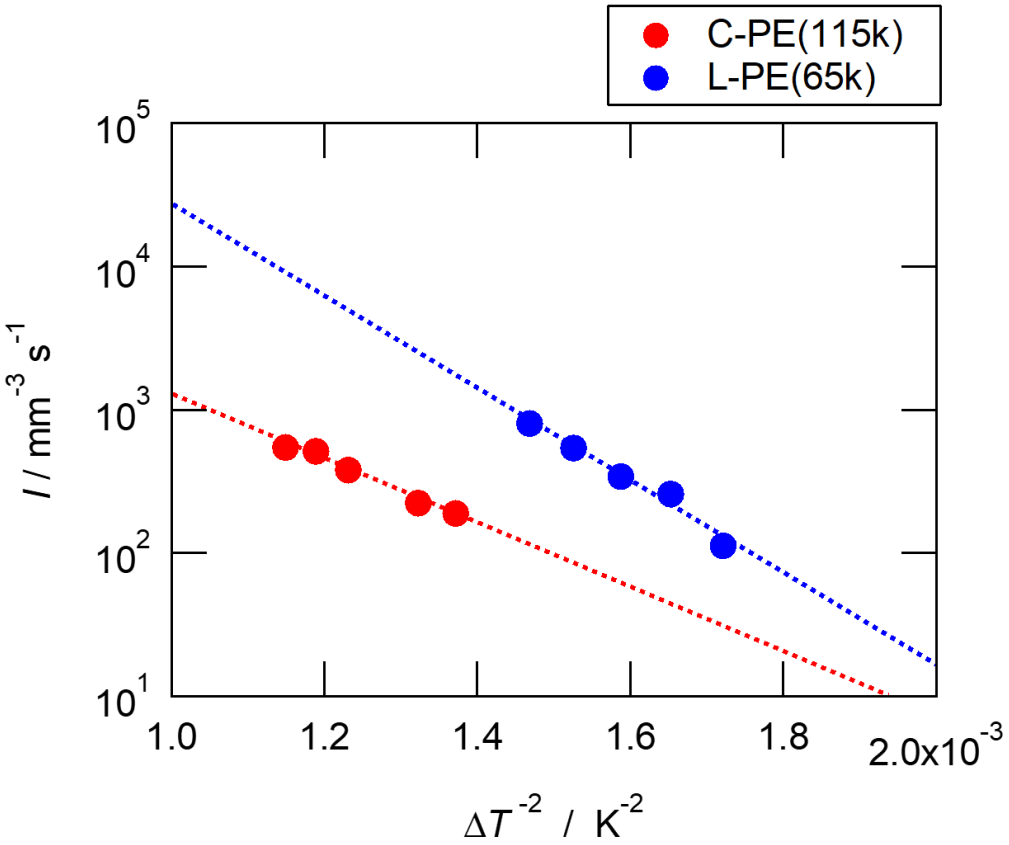

Figure 2.3 Plots of I against ΔT^{-2} for C-PE(115k) and L-PE(65k).

2-3-3 Formation mechanism of shish-like fibril crystals of C-PE and L-PE

Figure 2.4 (a) shows a schematic illustration of the initial formation process of a shish from the oriented melt of a general linear polymer. An oriented melt is formed when polymer chains are elongated at entanglement points by the applied flow to the polymer melt. The bundle nucleus is generated from this oriented melt and then grows into a shish-like fibril crystal.

Roovers previously reported that the entanglement density (ν_e) of linear polymers is five times larger than that of cyclic polymers with the same molecular weight [19]. Considering the difference in M_w between C-PE(115k) and L-PE(65k), it can be estimated that the ν_e of C-PE(115k) is two-fifths that of L-PE(65k). It is natural to consider that entanglement enhances the formation of oriented melt and suppresses crystallization. The density of the oriented melt is expected to be proportional to the entanglement density. Although it was reported that I_0 is exponentially controlled by ν_e [37], it does not lead to serious problems when considering that I_0 is linearly suppressed by ν_e, within a small change in ν_e. Therefore, it is assumed that the formation rate or formation density of shish-like fibril crystals is solely controlled by ν_e. However, the ten-fold difference in I_0 between C-PE(115k) and L-PE(65k) is excessively large to match the above assumption, implying that it is necessary to consider the entanglement density and entanglement species.

Figure 2.4 (b) shows a schematic illustration of the difference in the formation ability of the oriented melt of cyclic and linear polymers. Linear polymers exhibit many knot entanglements that have a functional pinning effect in the polymer network. By contrast, cyclic polymers have lower entanglements, including knot entanglement, than linear polymers due to the lack of chain ends. Moreover, the lack of knot entanglement makes it easier to disentangle compared to a linear polymer. Even if the cyclic polymer chains are stretched by external flow, they can easily relax to the state of randomly coiled chains. Therefore, it is more difficult for a cyclic polymer to form an oriented melt than a linear polymer. This is the reason why it is more difficult for C-PE to form shish-like fibril crystals than L-PE.

(a)

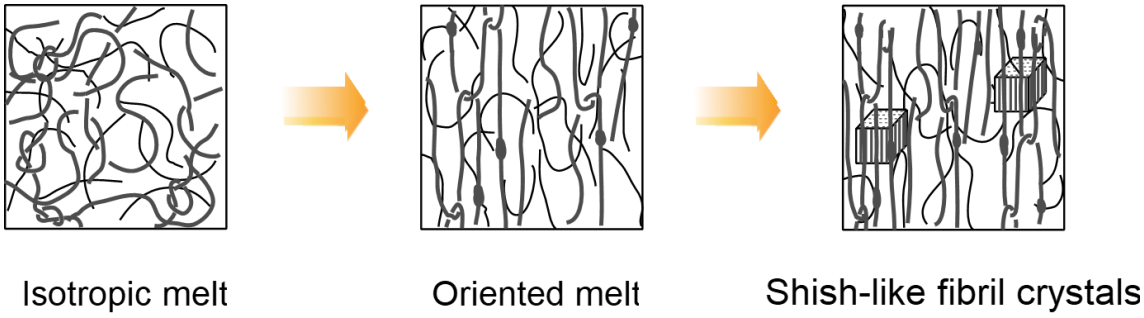

(b)

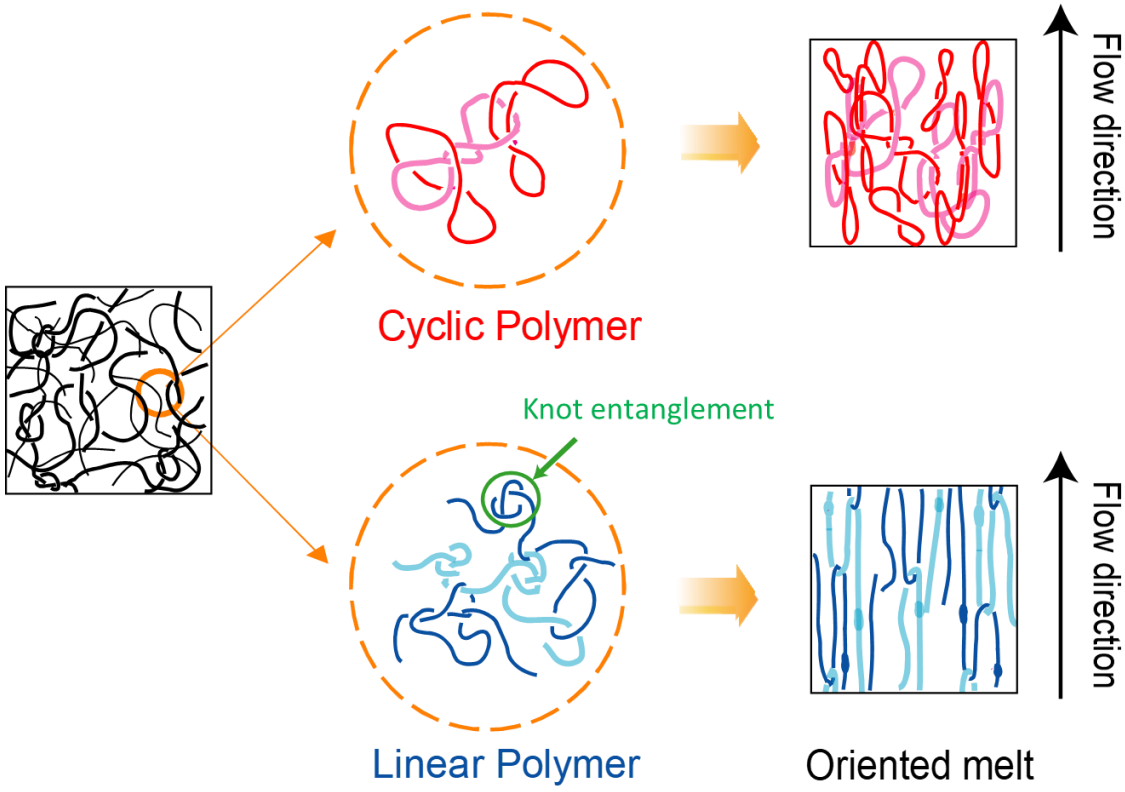

Figure 2.4 (a) Schematic illustration of the formation mechanism of shish-like fibril crystals. (b) Schematic illustration of the difference in the formation ability of the oriented melt between cyclic and linear polymers.

2-3-4 Effect of the addition of L-PE to C-PE

Further investigation of the effects of the entanglement species on the formation of shish-like fibril crystals was conducted using a blended sample of C-PE and L-PE. It has been reported that the addition of small amounts of linear chains to cyclic chains influences the crystallization rate in the quiescent state [38]. **Figure 2.5** shows plots of I against T_c for C-PE(115k), L-PE(65k), and blended samples of C-PE(44k) and L-PE(65k) with $\Phi_{L\text{-}PE}$ = 1 and 3 wt%. Notably, the C-PE(44k) homopolymer cannot form shish-like fibril crystals in this T_c range under the present shear conditions. The blended samples can easily form shish-like fibril crystals because the T_c range of the formation of the shish-like fibril crystals of the blended samples approaches that of the L-PE(65k) homopolymer, that is, a higher T_c range. In other words, the addition of small amounts of L-PE to C-PE remarkably enhances the formation of shish-like fibril crystals.

There is a concern that the enhancement of I in the blended samples may be caused by the formation of shish-like fibril crystals from only the L-PE component in the blended samples. **Figure 2.6** shows plots of ν_{st} against T_c for L-PE(65k) and the blended sample of C-PE(44k) and L-PE(65k) with $\Phi_{L\text{-}PE}$ = 3 wt%. Comparing ν_{st} at the same T_c, the ν_{st} of the blended sample was found to be approximately one-sixth that of the L-PE(65k) homopolymer. Because C-PE and L-PE have good compatibility with each other, it is expected that C-PE molecules are distributed uniformly within the matrix of L-PE. If only the L-PE component in the blended sample forms shish-like fibril crystals, it is not possible to reach such a high ν_{st} for the blended sample due to the small $\Phi_{L\text{-}PE}$ of 3 wt%. It is considered that the remarkable enhancement in the formation of shish-like fibril crystals is caused by the novel entanglement formed between C-PE and L-PE. **Figure 2.7** shows a schematic illustration of the formation of shish-like fibril crystals from the melt

of the C-PE homopolymer and blended samples of C-PE and L-PE. When C-PE with insufficient M_w is applied to the external flow, the C-PE chains are stretched incompletely, and some chains are immediately relaxed to a random coil. Consequently, it is difficult to form shish-like fibril crystals from these melts. By contrast, in the blended sample, the L-PE chain penetrates the C-PE ring [38]. This entanglement is not expected to easily disentangle. If an external flow is applied to such a melt, the chains will be strongly stretched, and shish-like fibril crystals will form easily compared to the C-PE homopolymer.

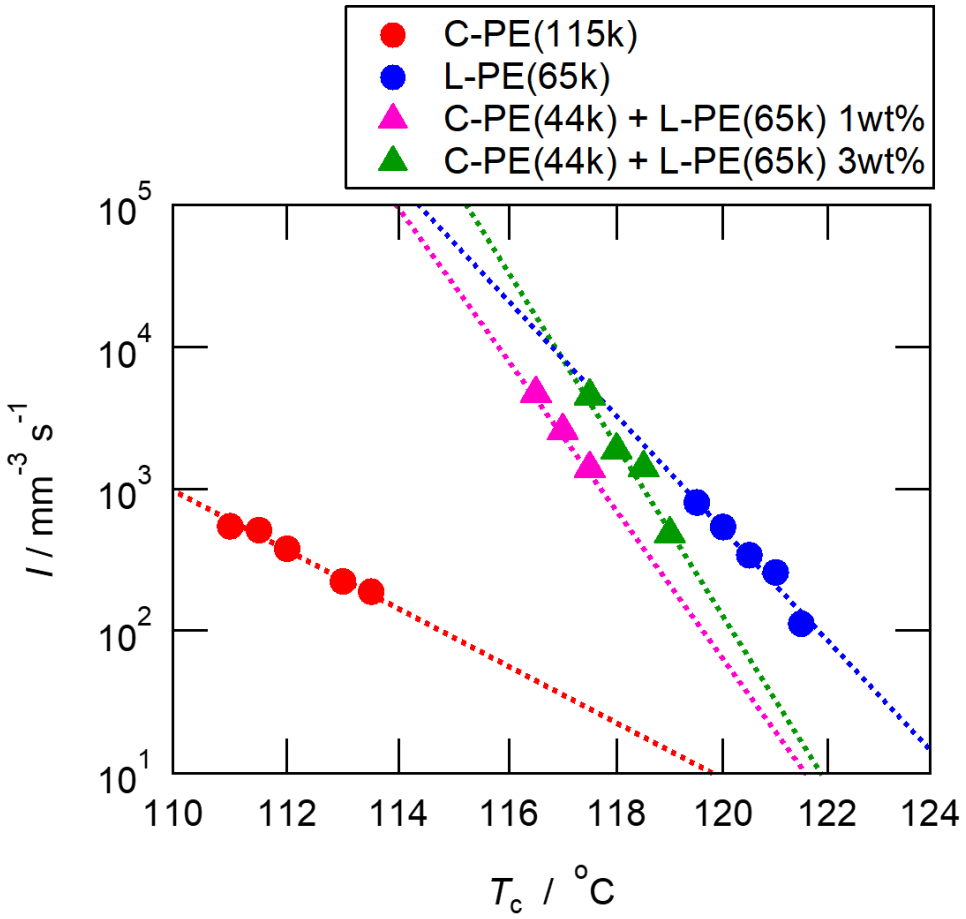

Figure 2.5 Plots of I against T_c for C-PE(115k), L-PE(65k), and blended samples of C-PE(44k) and L-PE(65k) with $\Phi_{L\text{-}PE}$ = 1 and 3 wt%.

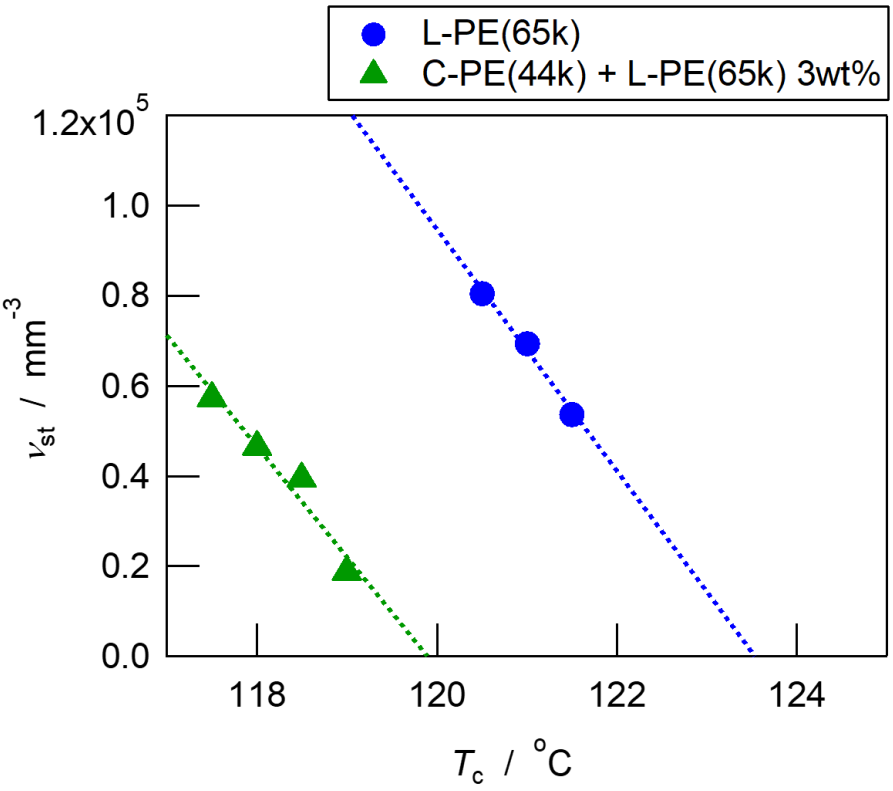

Figure 2.6 Plots of ν_{st} against T_c for L-PE(65k) and blended samples of C-PE(44k) and L-PE(65k). The $\Phi_{L\text{-}PE}$ in the blended sample was fixed at 3 wt%.

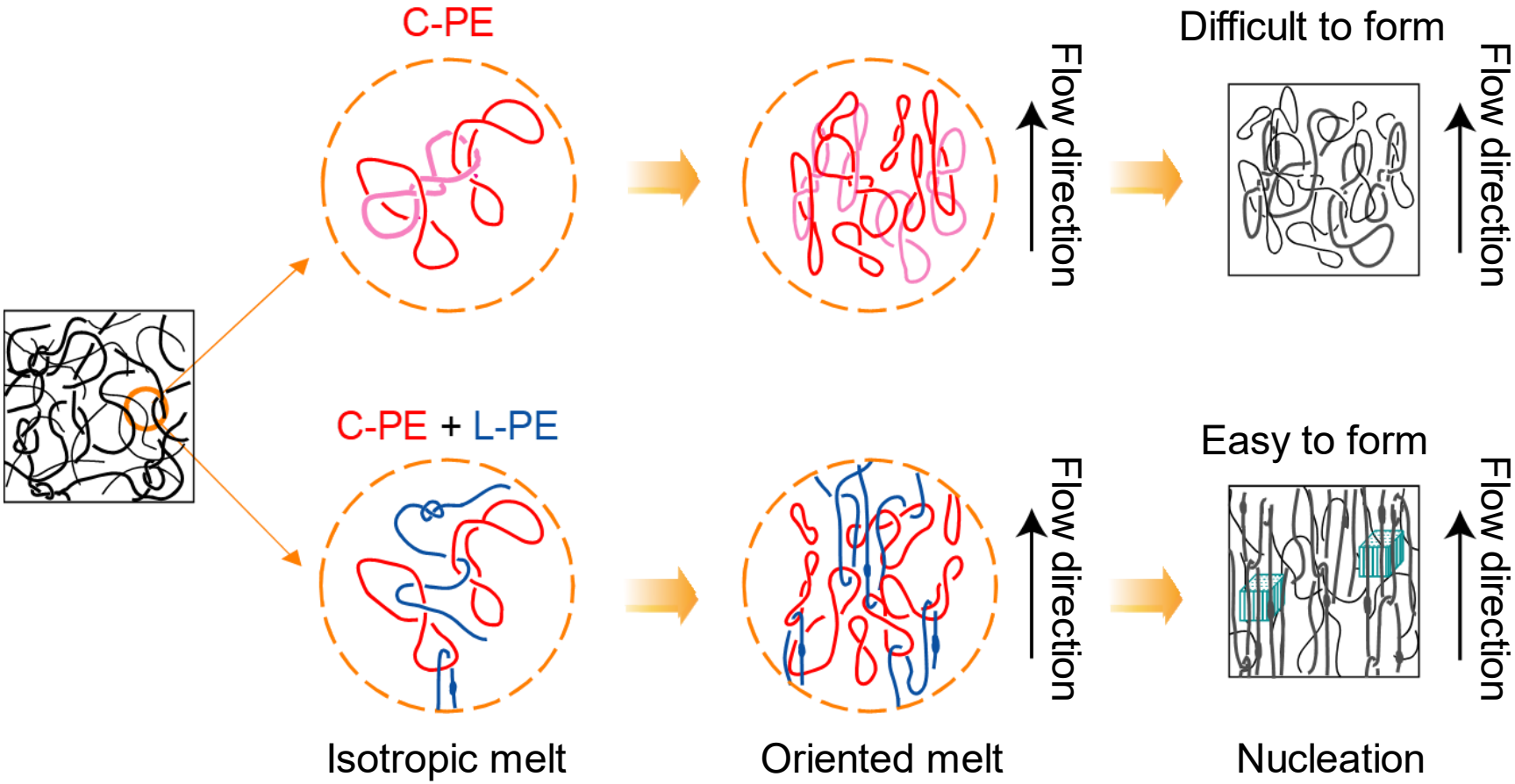

Figure 2.7 Schematic illustration of the effects of entanglements of neat C-PE and blended samples of C-PE and L-PE.

2-4 Conclusion

To clarify the effects of entanglement species on the formation of shish-like fibril crystals, the formation rate, I, of cyclic and linear polyethylenes (C-PE and L-PE, respectively) from the melt under pulsed shear flow ($\dot{\gamma}$ = 50 s^{-1} for 1 s) was studied as a function of the crystallization temperature, T_c, or the degree of supercooling, ΔT, using a POM. The C-PE(115k or 44k) and L-PE(65k) were prepared with weight average molecular weights, M_w, of 115000, 44000, and 65000, respectively. The I of the C-PE(115k) and L-PE(65k) homopolymers obeyed the equation $I = I_0\exp(-C/\Delta T^2)$. The values of C for the two samples were not very different. However, the I_0 of C-PE(115k) was significantly lower than that of L-PE(65k). This implies that the shish-like fibril crystals of C-PE are more difficult to form than those of L-PE. It was found that knot entanglement plays an important role in the formation of shish-like fibril crystals.

The shear-induced crystallization behavior of the blended C-PE and L-PE samples provided further insight into the effect of entanglement species on the formation of shish-like fibril crystals. The addition of small amounts of L-PE to the C-PE matrix significantly enhanced the formation of the shish-like fibril crystals. It is speculated that the novel entanglement formed by the penetration of the L-PE molecule into the C-PE ring affected the formation of the oriented melt.

2-5 References

[1] Keller A, Machin M J. Oriented crystallization in polymers. J Macromol Sci Part B. 1967;1:41–91.

[2] Pennings A J, Kiel A M. Fractionation of polymers by crystallization from solution, III. On the morphology of fibrillar polyethylene crystals grown in solution. Kolloid Z Z

Polym. 1965;205:160–162.

[3] Pennings A J, van der Mark J M A A, Kiel A M. Hydrodynamically induced crystallization of polymers from solution. Colloid Polym Sci. 1970;237:336–58.

[4] Mitsuhashi S. On polyethylene crystals grown from flowing solutions in xylene. Bull Text Res Inst (J). 1963;66:1–9.

[5] Bashir Z, Odell J A, Keller A. Stiff and strong polyethylene with shish kebab morphology by continuous melt extrusion. J Mater Sci. 1986;21:3993–4002.

[6] Liedauer S, Eder G, Janeschitz-Kriegl H, Jerschow P, Geymayer W, Ingolic E. On the kinetics of shear-induced crystallization in polypropylene. Int Polym Process. 1993;8:236–244.

[7] Keller A, Kolnaar H W H. Flow induced orientation and structure formation. In: Meijer H (ed) Processing of polymers. Wiley-VCH, Weinheim. 1997;18:189–268.

[8] Lieberwirth L, Loos J, Petermann J, Keller A. Observation of shish crystal growth into nondeformed melts. J Polym Sci Part B: Polym Phys. 2000;38:1183–1187.

[9] Somani R H, Yang L, Zhu L, Hsiao B S. Flow-induced shish-kebab precursor structures in entangled polymer melts. Polymer. 2005;46:8587–8623.

[10] Kumaraswamy G, Kornfield J A, Yeh F, Hsiao B S. Shear-enhanced crystallization in isotactic polypropylene. 3. Evidence for a kinetic pathway to nucleation. Macromolecules. 2002;35:1762–1769.

[11] Yamazaki S, Watanabe K, Okada K, Yamada K, Tagashira K, Toda A, Hikosaka M. Formation mechanism of shish in the oriented melt (I)-bundle nucleus becomes to shish. Polymer. 2005;46:1675–1684.

[12] Yamazaki S, Watanabe K, Okada K, Yamada K, Tagashira K, Toda A, Hikosaka M. Formation mechanism of shish in the oriented melt (II)-two different growth mechanisms

along and perpendicular to the flow direction. Polymer. 2005;46:1685–1692.

[13] Kanaya T, Matsuba G, Ogino Y, Nishida K. Hierarchic structure of shish-kebab by neutron scattering in a wide Q range. Macromolecules. 2007;40:3650–3654.

[14] Li K, Matsuba G. Effects of relaxation time and zero shear viscosity on structural evolution of linear low-density polyethylene in shear flow. J Appl Polym Sci. 2018;135:46053.

[15] de Gennes P G. Tight knots. Macromolecules. 1984;17:703–703.

[16] Iwata K. Role of entanglement in crystalline polymers 1. Basic theory. Polymer. 2002;43:6609–6626.

[17] Rastogi S, Lippits D R, Peters G W M, Graf R, Yao Y, Spiess H W. Heterogeneity in polymer melts from melting of polymer crystals. Nat Mater. 2005;4:635–641.

[18] Yamazaki S, Gu F, Watanabe K, Okada K, Toda A, Hikosaka M. Two-step formation of entanglement from disentangled polymer melt detected by using nucleation rate. Polymer. 2006;47:6422–6428.

[19] Roovers J. Viscoelastic properties of polybutadiene rings. Macromolecules. 1988;21:1517–1521.

[20] Gratton Y, Slater G W. Molecular dynamics study of tethered polymers in shear flow. Eur Phys J E. 2005;17:455–465.

[21] Bielawski C W, Benitez D, Grubbs R H. An “Endless” route to cyclic polymers. Science. 2002;297:2041–2044.

[22] Fürstner A, Ackermann L, Gabor B, Goddard R, Lehmann C W, Mynott R, Stelzer F, Thiel O R. Comparative investigation of ruthenium-based metathesis catalysts bearing *N*-heterocyclic carbene (NHC) ligands. Chem Eur J. 2001;7:3236–3253.

[23] Kobayashi K, Yamazaki S, Kimura K. Formation of shish-like fibril crystals from

the melt of blends of cyclic and linear polyethylene under shear flow. Polym J. 2022;54:913–920.

[24] Wunderlich B, Czornyj G. A study of equilibrium melting of polyethylene. Macromolecules. 1977;10:906–913.

[25] Broadhurst M G. Extrapolation of the orthorhombic *n*-paraffin melting properties to very long chain lengths. J Chem Phys. 1962;36:2578–2581.

[26] Broadhurst M G. The melting temperatures of the *n*-paraffins and the convergence temperature for polyethylene. J Res Natl Bur Stand A. 1966;70:481–486.

[27] Ogino Y, Fukushima H, Matsuba G, Takahashi N, Nishida K, Kanaya T. Effects of high molecular weight component on crystallization of polyethylene under shear flow. Polymer. 2006;47:5669–5677.

[28] Pennings A J. Fractionation of polymers by crystallization from solutions. II. J Polym Sci Part C: Polym Sympo. 2007;16:1799–1812.

[29] Yamazaki S, Hikosaka M, Toda A, Wataoka I, Yamada K, Tagashira K. Nucleation and morphology of polyethylene under shear flow. J Macromol Sci Part B. 2003;42:499–514.

[30] Wunderlich B. Macromolecular physics. Vol 3. Crystal melting. Academic Press: New York; 1980.

[31] Yamazaki S, Itoh M, Oka T, Kimura K. Formation and morphology of “shish-like” fibril crystals of aliphatic polyesters from the sheared melt. Eur Polym J. 2010;46:58–68.

[32] Turnbull D, Fisher J C. Rate of nucleation in condensed systems. J Chem Phys. 1949;17:71–73.

[33] Price F P. Nucleation in polymer crystallization. In: Zettlemoyer A C, editor. Nucleation. Marcel Dekker: New York; 1969.

[34] Umemoto S, Hayashi R, Kawano R, Kikutani T, Okui N. Molecular weight dependence of primary nucleation rate of poly(ethylene succinate). J Macromol Sci Part B. 2003;42:421–430.

[35] Nishi M, Hikosaka M, Ghosh S K, Toda A, Yamada K. Molecular weight dependence of primary nucleation rate of polyethylene I. An extended chain single crystal. Polym J. 1999;31:749–758.

[36] Ghosh S K, Hikosaka M, Toda A, Yamazaki S, Yamada K. Power law of molecular weight of the nucleation rate of folded chain crystals of polyethylene. Macromolecules. 2002;35:6985–6991.

[37] Yamazaki S, Hikosaka M, Toda A, Wataoka I, Gu F. Role of entanglement in nucleation and 'melt relaxation' of polyethylene. Polymer. 2002;43:6585–6593.

[38] López J V, Pérez-Camargo R A, Zhang B, Grayson S M, Müller A J. The influence of small amounts of linear polycaprolactone chains on the crystallization of cyclic analogue molecules. RSC Adv. 2016;6:48049–48063.

[39] Ruiz M B, Pérez-Camargo R A, López J V, Penott-Chang E, Múgica A, Coulembier O, Müller A J. Accelerating the crystallization kinetics of linear polylactides by adding cyclic poly (L-lactide): Nucleation, plasticization and topological effects. Int J Biol Macromol. 2021;186:255–267.

Chapter 3

Formation of shish-like fibril crystals from the melt of blends of cyclic and linear polyethylene under shear flow

3-1 Introduction

3-1-1 Effect of entanglements of linear polyolefins on shear-induced crystallization

When linear polyolefins such as polyethylene (PE) and polypropylene (PP) are subjected to shear flow, the molecular chains of the linear polyolefins are elongated, and an oriented melt is formed. Subsequently, precursors of extended chain crystals, also known as shish crystals, are formed from the oriented melt. The precursors grow to shish or shish-like fibril crystals, and folded chain lamellar crystals (kebab crystals) are epitaxially generated on the surface of the shish [1–8]. Several possible models, such as the Janeschitz-Kriegl model [9–13], coil-stretch model by Keller et al. [14,15], and Petermann model [16], have been proposed for the formation of shish-kebab crystals, and their formation mechanisms have been discussed. Since the shish-kebab structure consists of the core of the extended chain crystal and epitaxially grown folded lamellar crystals, it is widely believed that the shish crystals should be formed before the kebab crystals [17–26]. However, Murase et al. recently proposed a new method for the formation of shish-kebab crystals using ultrahigh molecular weight PE (UHMWPE) via gel-spinning [27–30]. Accordingly, the formation mechanism of shish-kebab crystals is still under debate. Blends of binary molecular weights have often been used to elucidate the formation mechanism of shish-kebab crystals. Fukushima et al. [31], Kanaya et al. [32], Yang et al. [33], and Kimata et al. [34] independently investigated the flow-induced crystallization of a PE blend with high and low molecular weights. Seki et al. [35] and Keum et al. [36]

independently studied the shear-induced crystallization of PP blends. In these studies, long-chain components have been shown to play an important role in the formation of a shish-kebab crystalline structure. Long-chain components become entangled with each other, and these entanglements enhance the chain stretching under the flow field. To summarize, these studies were performed to clarify the role of entanglements in the formation of the shish-kebab structure. Although the importance of entanglements in the formation of the shish-kebab structure has been frequently reported, as mentioned above, it has not yet been fully studied and is not yet understood.

3-1-2 Crystallization of cyclic and linear polymers

Cyclic polymers are topologically different from linear polymers because of the absence of chain ends; therefore, they show lower entanglements and faster self-diffusion than linear polymers. Several pioneering experimental studies have been conducted on the physical properties of cyclic polymers with the evolution of synthetic methods. Roovers showed the viscoelastic properties of cyclic polystyrene and polybutadiene in a melt [37,38]. McKenna et al. also demonstrated that cyclic polystyrenes have a lower melt viscosity than linear ones [39,40]. These results are understood by the lower entanglements of the cyclic polymer relative to the linear polymer. Thus, the crystallization behaviors of cyclic polymers differ from those of linear polymers. Córdova et al. and Su et al. reported the crystal growth of cyclic and linear poly(ε-caprolactone) (PCL) from a melt in a quiescent state [41,42]. They showed that the spherulitic growth rates of cyclic PCL are approximately one order of magnitude higher than those of linear PCL at the same crystallization temperature (T_c) when cyclic and linear PCLs have an almost identical weight average molecular weight (M_w). Shin et al. also showed that cyclic

PCL has a lower half-crystallization time than linear PCL [43]. The faster crystallization of cyclic PCL compared to linear PCL, when M_w exceeded 75,000 g/mol, was considered to be influenced by the topological characteristics of cyclic PCL, such as lower entanglements. Cyclic PCL was considered to have a higher rate of crystallization than linear PCL because of its faster disentangling within the melt. In contrast, results that were opposite to those mentioned above have also been reported, and the possibility that experimental facts cannot be explained by entanglements alone has been suggested several times [44–46]. The current conflict on the crystal growth of cyclic polymers has been comprehensively summarized by Pérez et al. [47].

As it is clear that the entanglements are closely related to the viscoelasticity or rheology of polymers [48], it is expected that the effect of entanglements on shear-induced crystallization may be remarkably greater than that on crystallization in the quiescent state mentioned above. Owing to the difficulties in preparing cyclic crystalline polymers with high purity and high yield, there are limited studies on the shear-induced crystallization of cyclic polymers. As described in Chapter 2, the shear-induced crystallization behavior of cyclic PE (C-PE) and linear PE (L-PE) homopolymers was compared [49]. It was found that C-PE formed shish-like fibril crystals from the sheared melt, as well as L-PE, when the M_w of C-PE was sufficiently high. The melting temperature (T_m) of the shish-like fibril crystals obtained from C-PE was significantly lower than that of crystals obtained from L-PE. The formation rate of shish-like fibril crystals (I) of C-PE was lower than that of L-PE. These results imply that the lack of entanglements, attributed to topological features associated with the absence of the C-PE chain end, suppressed the formation of shish-like fibril crystals for C-PE in shear-induced crystallization. It was also reported the shear-induced crystallization of a PE blend of C-PE as the matrix and L-PE as an additive.

The formation of shish-like fibril crystals for the PE blend was accelerated by the addition of L-PE to the C-PE matrix. Mills et al. reported the unique diffusion behavior of cyclic polymers in a linear polymer matrix [50]. These results imply the influence of novel entanglement species formed by cyclic and linear polymers.

3-1-3 Purpose of this chapter

In this chapter, the formation of shish-like fibril crystals of blend samples with C-PE as a matrix and L-PE as an additive in shear-induced crystallization was clarified. The M_w and blend ratios of C-PE and L-PE were changed to control the entanglement density, and the effect of the entanglement state formed by C-PE and L-PE on the formation of shish-like fibril crystals will be investigated.

3-2 Experimental

3-2-1 Samples

The C-PE and L-PE were prepared using the same procedures reported previously [51–54]. PE precursors such as cyclic and linear polyoctenamers were synthesized via the ring-opening metathesis polymerization of *cis*-cyclooctene catalyzed by a cyclic Ru-alkylidene complex and second-generation Grubbs catalyst, respectively. Both PE precursors were hydrogenated with *p*-toluenesulfonyl hydrazide and converted to the corresponding PE. The chemical structures of the samples were confirmed by FT-IR (JASCO FT/IR-410 spectrometer), ^{1}H NMR, and ^{13}C NMR (JEOL AL300 SC-NMR). The M_w of the L-PEs was also calculated assuming 100% hydrogenation of L-PO. The M_w of C-PO and L-PO was evaluated using the relationship between the intrinsic viscosity and M_w reported by Bielawski et al. [51]. The M_w values of C-PE and L-PE used in this

chapter are summarized in **Table 3.1**.

Blended samples of C-PE and L-PE for shear-induced crystallization were prepared as follows; the C-PE and L-PE homopolymers were mixed in a predetermined fraction and completely dissolved in *o*-xylene. The solution was poured into excess methanol, and the precipitate was recovered from the solution. The powder-blended samples were fully dried in vacuo. The four types of blended samples prepared in this chapter are summarized in **Table 3.2**. Hereafter, the weight fraction of L-PE in the blended sample is referred to as $\Phi_{\text{L-PE}}$. Before the observation of shear-induced crystallization, all samples were first melted above the equilibrium melting temperature (T_m^0) under an Ar atmosphere and then quenched ca. 20 °C to prepare a film-like sample. The T_m^0 of C-PE and L-PE were estimated assuming that the T_m^0 of C-PE is equal to that of perfectly extended chain crystals of linear polymethylene that possess half the M_w of C-PE [55]. However, for L-PE, the relation between T_m^0 and the carbon number of the linear PE in the backbone was applied, as reported by Broadhurst [56,57]. The calculated T_m^0 values of C-PE and L-PE are also summarized in **Table 3.1**.

Table 3.1 M_w and T_m^0 of C-PE and L-PE used in this chapter.

Code	M_w / g mol^{-1}	T_m^0 / °C
C-PE(230k)	232×10^3	141.0
C-PE(130k)	130×10^3	140.9
C-PE(86k)	86×10^3	140.7
L-PE(104k)	104×10^3	145.9
L-PE(42k)	42×10^3	145.1

Table 3.2 Experimental conditions of the blend samples.

Component		$\dot{\gamma}$ / s^{-1}	t_d / s	ε / -	T_c / °C
C-PE(230k)	L-PE(42k)	30	1	30	120
C-PE(130k)	L-PE(42k)	70	1	70	119
C-PE(86k)	L-PE(42k)	70	1	70	119
C-PE(230k)	L-PE(104k)	5	1	5	120

3-2-2 Instruments and measurements

The behavior of shear-induced crystallization was observed using a hot stage (Linkam, CSS-450) equipped with a polarizing optical microscope (POM, Olympus, BX-51). The geometry of the hot stage consisted of a quartz parallel plate rotating the bottom plate. The gap between the two plates was fixed at 100 μm. In shear-induced crystallization, the film-like samples were heated to 160 °C (T_{max}) at a heating rate of 30 °C/min and were melted completely. The molten state was maintained at T_{max} for 1 min to erase the thermal history of the samples. Then, the samples were cooled and isothermally crystallized at the crystallization temperature (T_c = 119–120 °C). The range of shear rate ($\dot{\gamma}$) was 5–70 s^{-1}, and the duration of shear flow (t_d) was fixed at 1 s. Therefore, the shear strain was different for each sample. The shear flow was applied just before T_c (ca. T_c+0.5 °C). Subsequently, the formation of shish-like fibril crystals from the quiescent melt was observed. As reported in a paper [23], the number density of shish-like fibril crystals (N) corresponds to that of the nuclei. A single nucleus grows into a shish in an earlier stage, following which the shish becomes overgrown, forming a strand-like structure (shish-like fibril crystal). the formation of an overgrown fibril crystal was observed using a POM in the early stages and was measured the number density of the

nuclei that grew to shish-like fibril crystals (N). The formation rate of shish-like fibril crystals, I, is defined by:

$$I \equiv \mathrm{d}N/\mathrm{d}t \tag{3.1}$$

where t is the crystallization time. In this chapter, it was found that N increases linearly with t and then saturates at a certain value (ν_{st}) (**Figures S3.1–S3.4** in the Appendix). it was adjusted the shear strain such that ν_{st} is almost of the same order for each sample (**Figures S3.5–S3.6** in the Appendix). The experimental conditions for shear-induced crystallization are summarized in **Table 3.2**.

3-3 Results and discussion

Figure 3.1 shows the typical morphologies of the shish-like fibril crystals for a) $\Phi_{L\text{-}PE}$ = 0 wt%, b) $\Phi_{L\text{-}PE}$ = 1 wt%, and c) $\Phi_{L\text{-}PE}$ =100 wt% of the C-PE(230k)/L-PE(42k) blend system observed by POM. As mentioned in the experimental section, to adjust ν_{st} to almost the same order for all the samples, T_c = 120 °C for $\Phi_{L\text{-}PE}$ = 0 and 1 wt% and T_c = 126 °C for $\Phi_{L\text{-}PE}$ = 100 wt% was chosen. In contrast, $\dot{\gamma}$, t_d, and shear strain ε (= $\dot{\gamma}\times t_d$) were fixed for all the samples. Therefore, the experimental conditions of shear-induced crystallization when $\Phi_{L\text{-}PE}$ = 100 wt% were milder than those of the other systems. In all the samples, similar morphologies of fibril crystals were demonstrated by the following authors: Ogino et al. for PP [58]; Zhao et al. for PP [59]; Yamazaki et al. for PE, PP, and aliphatic polyesters [23,24,60,61]; Pennings for PE and PP [62]; and Wang et al. for branched PLLA [63]. The T_m of the shish-like fibril crystals was significantly higher than that of spherulite, which is a folded chain crystal and is close to the T_m^0 of PE [49]. This result indicates that the lamellar thickness of shish-like fibril crystals is larger than that of spherulites, as predicted by the Gibbs–Thomson equation [64], and is close to that of the

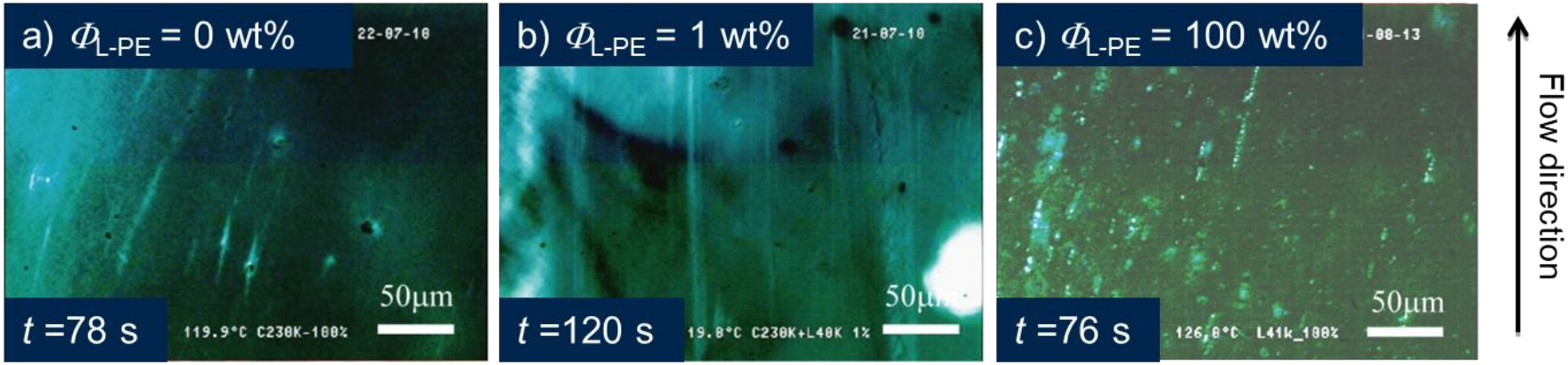

Figure 3.1 Polarizing optical micrographs of shish-like fibril crystals formed from the sheared melt of the C-PE(230k)/L-PE(42k) blend system with a) $\Phi_{L\text{-}PE}$ = 0 wt%, b) $\Phi_{L\text{-}PE}$ = 1 wt% and c) $\Phi_{L\text{-}PE}$ = 100 wt%.

extended chain crystal.

Although it is necessary to conduct detailed observations such as by transmitted or scanning electron microscopy (TEM or SEM) for the morphologies obtained in this chapter, it is assumed that a single strand of the shish-kebab crystals become overgrown, forming shish-like fibril crystals, as concluded by Yamazaki et al. [23,24,60,61]. Despite the milder crystallization conditions for $\Phi_{\text{L-PE}}$ = 100 wt% compared to the others, the number of shish-like fibril crystals formed was qualitatively comparable among these samples. Additionally, the M_w of L-PE in this blend was significantly smaller than that of C-PE. Therefore, L-PE can form shish-like fibril crystals more easily than C-PE. In the blend system of C-PE and L-PE, each component is not expected to crystallize separately from the sheared melt. From the observations of the molten state of all the blend samples by POM, macroscopic phase separation was not observed. As reported by Fukushima et al. [31], Kanaya et al. [32], and Yang et al. [33], the binary blend of PE with a large M_w difference could not be interpreted as the segregated shear-induced crystallization of each component. Additionally, as reported by An et al. [65], even in topologically different blend systems of linear PE and branched PE, segregated shear-induced crystallization cannot be expected. From these analogies, it is considered that segregated shear-induced crystallization does not occur in topologically different blend systems of cyclic and linear polymers used in this chapter.

Figure 3.2 shows the $\Phi_{\text{L-PE}}$ dependence of I in the C-PE(230k)/L-PE(42k) and C-PE(230k)/L-PE(104k) blend systems, where the M_w of C-PE is relatively high. The shear conditions of both blend samples were different. When the latter sample was measured with the same shear conditions as the former sample, I of the latter sample was not in the observable range and became extremely large. In both blend systems, a maximum in I

was observed against $\Phi_{L\text{-}PE}$. In contrast, it seems that $\Phi_{L\text{-}PE}^{*}$, where I reached a maximum, was maintained around $\Phi_{L\text{-}PE}$ = 1 wt% in both blend systems. In the former system, I at $\Phi_{L\text{-}PE}$ = 0 wt% was not much larger than that in the latter system. This result is reasonable because the latter system was under milder shear conditions than the former system. The remarkably small difference in I at $\Phi_{L\text{-}PE}$ = 0 wt% may imply that the formation of shish-like fibril crystals, in the case of the C-PE homopolymer, is not sensitive to the shear conditions because there were fewer entanglements of C-PE relative to L-PE.

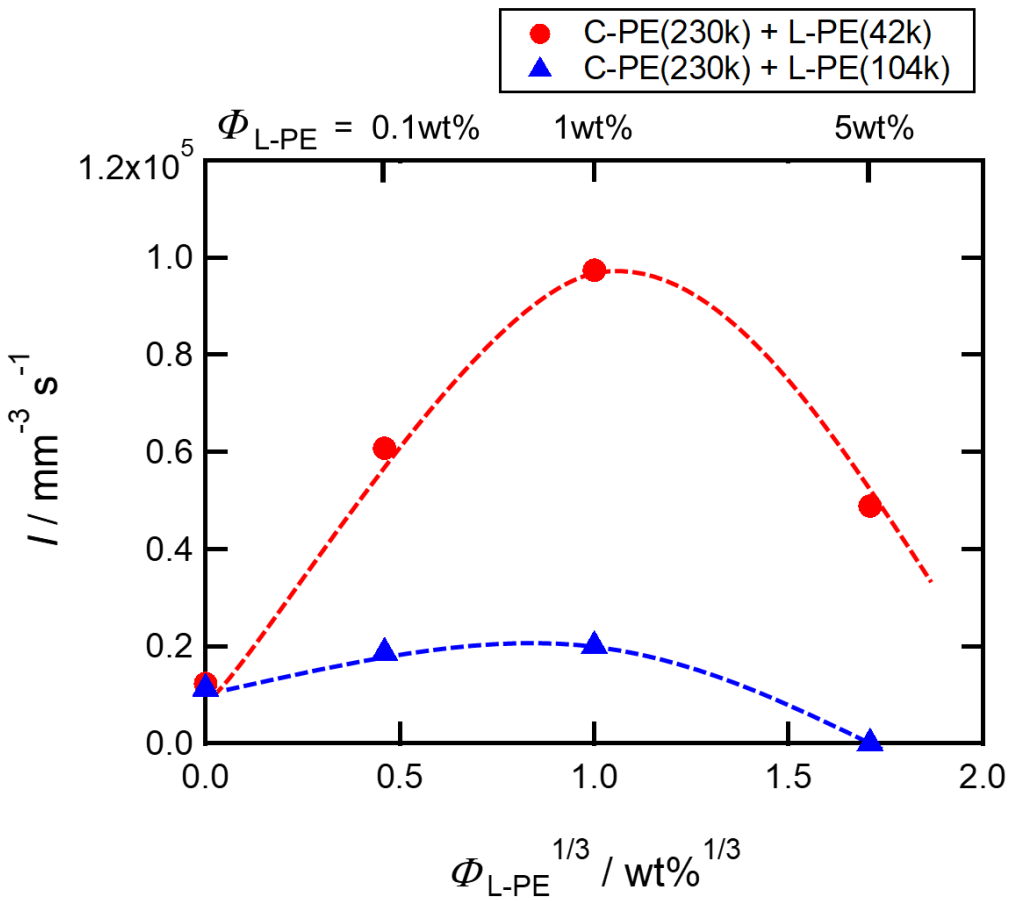

Figure 3.2 Plots of the formation rate of shish-like fibril crystals I vs. $\Phi_{L\text{-}PE}$ in the C-PE(230k)/L-PE(42k) and C-PE(230k)/L-PE(104k) blend systems.

In these blend systems, the M_w of C-PE is sufficiently large to form shish-like fibril crystals [49]. As noted by Roovers [37,38], it is expected that C-PE with a high M_w has the necessary number of entanglements to stretch the chains under shear flow, although the entanglement density of C-PE is smaller than that of L-PE. In shear-induced crystallization, two competing factors are attributed to entanglement, the enhancement of the formation of the oriented melt and the suppression of crystallization, as shown in **Figure 3.3**. The increase and decrease in the entanglement density correspond to the increase and decrease of $\Phi_{\text{L-PE}}$. While the former increased the formation rate of shish-like fibril crystals, the latter caused it to decrease. Because the increase in the entanglement density due to the addition of L-PE enhances the formation of the oriented melt and suppresses crystallization, an appropriate entanglement density exists for the formation of shish-like fibril crystals. The entanglement density increases with increasing $\Phi_{\text{L-PE}}$ because L-PE has free groups at both ends that can entangle with other chains. In both blend systems, with increasing $\Phi_{\text{L-PE}}$, the enhancement of the formation of the oriented melt becomes dominant during chain stretching under shear flow, as shown in the second row of **Figure 3.3**. This facilitated the formation of shish-like fibril crystals. Subsequently, in the nucleation and growth stages, excess large $\Phi_{\text{L-PE}}$, that is, a high entanglement density, suppressed the nucleation of shish-like fibril crystals, as shown in the third row of **Figure 3.3**. This made the formation of shish-like fibril crystals difficult, thereby maximizing the $\Phi_{\text{L-PE}}$ dependence of I. Finally, the change in I at approximately $\Phi_{\text{L-PE}} = 1$ wt% for both blend systems may be related to the concentration of overlapping L-PE in the bulk (ca. 1 wt%).

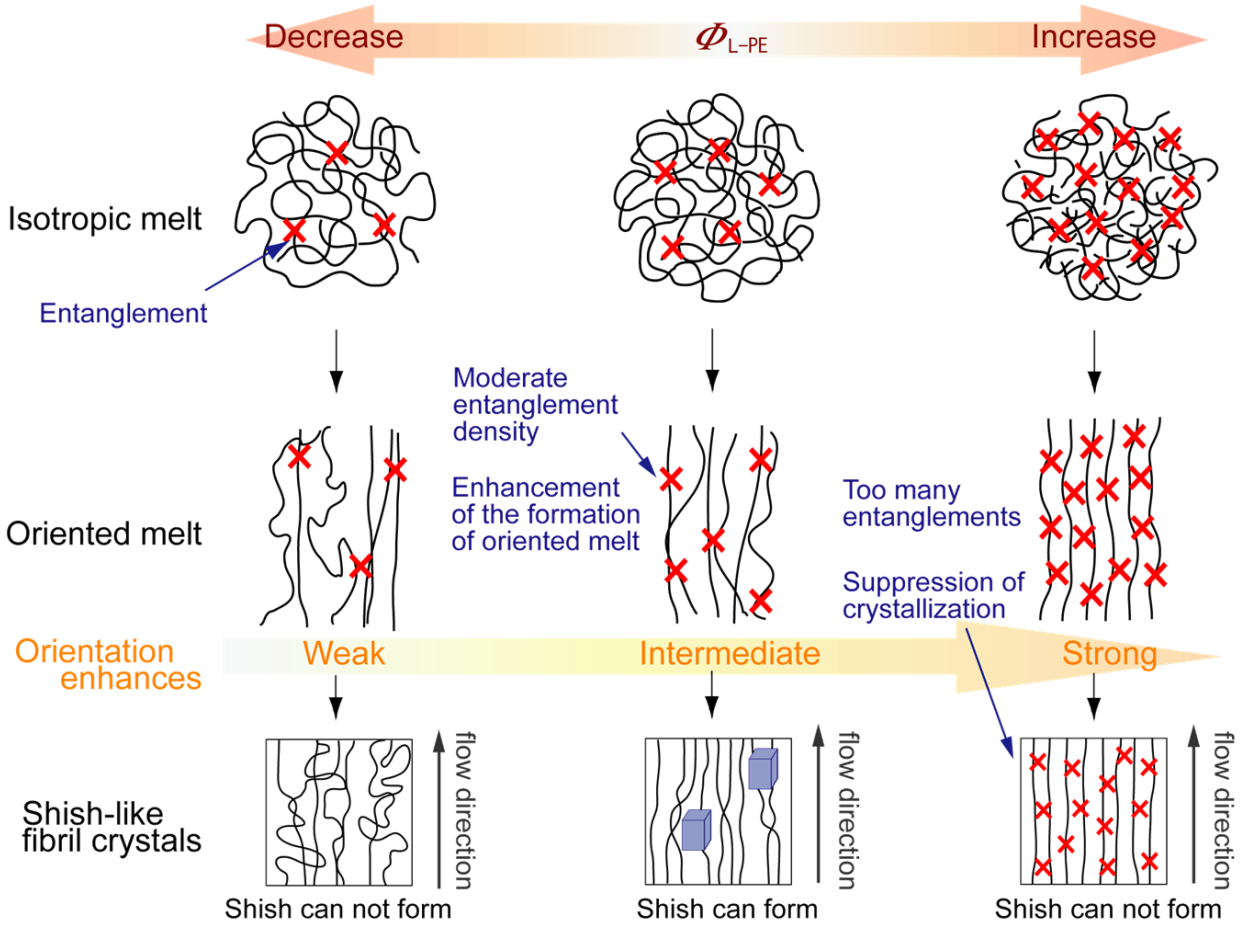

Figure 3.3 Schematic illustration of the effects of entanglements on the formation of the oriented melt and the suppression of crystallization.

Figure 3.4 shows the $\Phi_{\text{L-PE}}$ dependence of I for the C-PE(230k)/L-PE(42k), C-PE(130k)/L-PE(42k), and C-PE(86k)/L-PE(42k) blend systems. The M_w of L-PE in these blend systems was fixed at a constant, that is, M_w = 42,000. However, the M_w of C-PE was variable. In these blend systems, the total entanglement density was less than that shown in **Figure 3.2** because of the lower M_w of each component. The absolute values of I among these blend systems should not be compared because the experimental conditions of the shear-induced crystallization were different, as mentioned previously. In C-PE(230k)/L-PE(42k), as shown in **Table 3.2**, T_c was slightly higher and $\dot{\gamma}$ was smaller than those in the other systems. In this system, the formation of shish-like fibril crystals was lower than that in the others over the entire range of $\Phi_{\text{L-PE}}$. This result is reasonable because this system was under the mildest experimental conditions for shear-induced crystallization. To compare the $\Phi_{\text{L-PE}}$ dependence of I among these samples, the experimental conditions (T_c and $\dot{\gamma}$) of shear-induced crystallization should be fixed against all $\Phi_{\text{L-PE}}$ and all these samples. However, although the T_c and $\dot{\gamma}$ of C-PE(130k)/L-PE(42k) and C-PE(86k)/L-PE(42k) are the same, they are different from those of C-PE(230k)/L-PE(42k). This means that the comparison of the $\Phi_{\text{L-PE}}$ dependence of I among these three samples should not be carried out directly. Therefore, it should be focused on the change in I in each blend system against $\Phi_{\text{L-PE}}$. For all these blend systems, I reached a maximum against $\Phi_{\text{L-PE}}$; however, $\Phi_{\text{L-PE}}{}^{*}$ was different. In the C-PE(130k)/L-PE(42k) and C-PE(86k)/L-PE(42k) blend systems, $\Phi_{\text{L-PE}}{}^{*}$ was almost identical, and there seems to be no clear M_w dependence of C-PE in the blend component. I reached a clear maximum in the C-PE(130k)/L-PE(42k) system, but it was somewhat ambiguous for C-PE(86k)/L-PE(42k). The unclear maximum in the latter system may be due to the lower entanglement density compared with that in the former. In contrast, in the C-PE(230k)/L-

PE(42k) blend system, $\Phi_{\text{L-PE}}{}^{*}$ was shifted to the larger $\Phi_{\text{L-PE}}$. The maximum presented in **Figure 3.4** can be interpreted using the mechanism shown in **Figure 3.3**. The reason for the shift in the maximum in **Figure 3.4** to a lower $\Phi_{\text{L-PE}}$ was investigated when the shear conditions became strong, such as those of the C-PE(130k)/L-PE(42k) and C-PE(86k)/L-PE(42k) blend systems. The experimental results showed that $\Phi_{\text{L-PE}}{}^{*}$ was not determined solely by the entanglement density within the samples. As has been reported by many researchers [66–73], when the shear conditions such as the shear rate or strain become strong, it is well known that the influence of shear quickly appears in an earlier stage of crystallization, for example, in the shortening of the induction period of nucleus formation or the increase in nucleation density. Even in the case of the addition of a small amount of L-PE, that is, a small increase in the entanglement density, the influence of shear is observed with the increase in shear strength. As a result, it is considered that the maximum of the C-PE(130k)/L-PE(42k) and C-PE(86k)/L-PE(42k) blend systems appeared at a lower $\Phi_{\text{L-PE}}$.

3-4 Conclusion

With polarized microscopic observations of blended samples of C-PE as a matrix and L-PE as an additive, the effect of the M_{w} and blend ratio of C-PE and L-PE on the formation rate of shish-like fibril crystals (I) was clarified. In all blend systems of C-PE(230k)/L-PE(42k), C-PE(230k)/L-PE(104k), C-PE(130k)/L-PE(42k), and C-PE(86k)/L-PE(42k), the maximum was observed at a certain weight fraction of L-PE, i.e., $\Phi_{\text{L-PE}}$. The increase in $\Phi_{\text{L-PE}}$ corresponded to an increase in the entanglement density, which promoted the formation of oriented melts. Additionally, the increase in $\Phi_{\text{L-PE}}$ led to the suppression of crystallization. These results imply that the formation of shish-like

fibril crystals in the blended samples of C-PE and L-PE was determined by these competing effects.

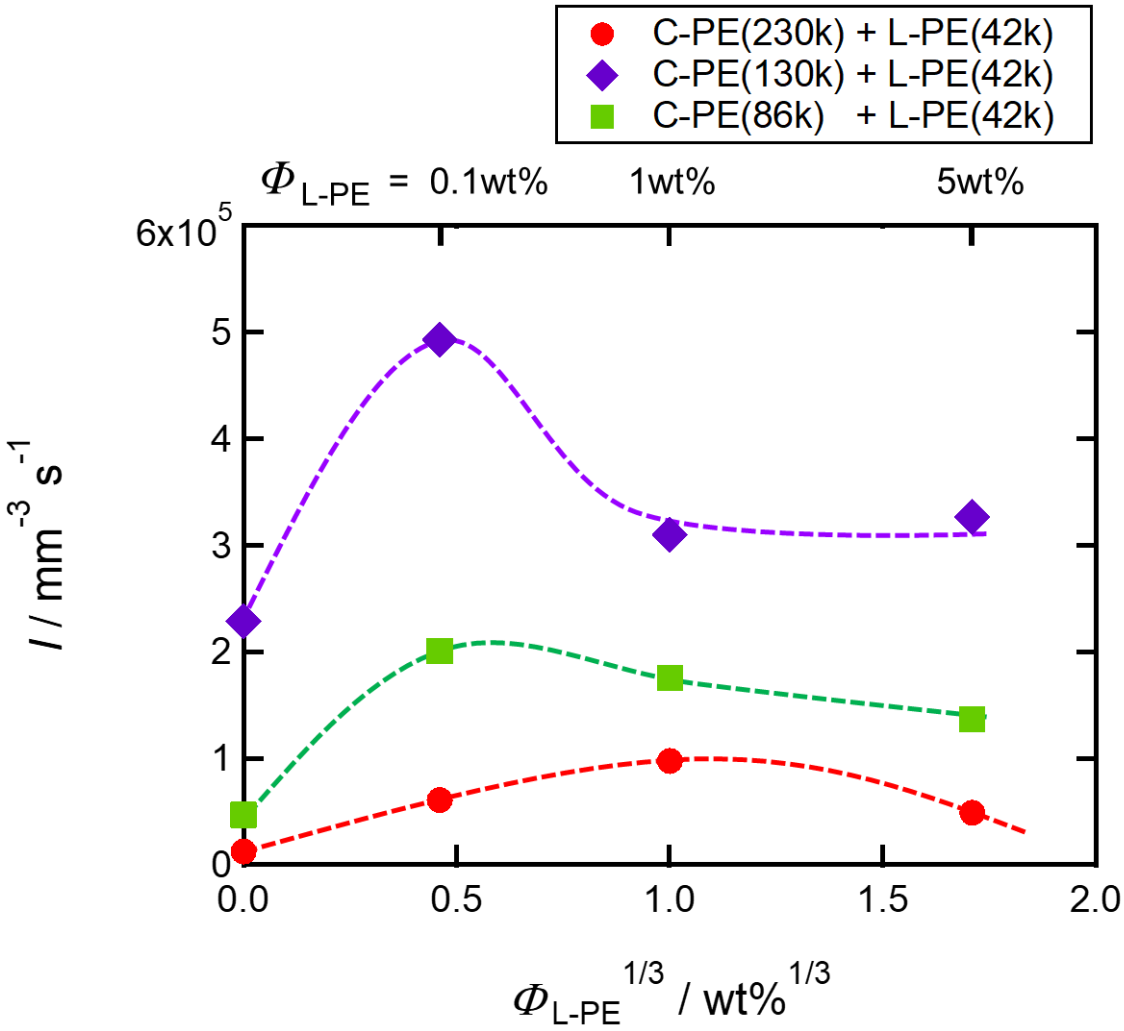

Figure 3.4 Plots of I vs. $\Phi_{\text{L-PE}}$ for C-PE(230k)/L-PE(42k), C-PE(130k)/L-PE(42k), and C-PE(86k)/L-PE(42k) blend systems.

3-5 Appendix

3-5-1 Row data of the number density of shish-like fibril crystals *N* vs. *t*

Figures S3.1–S3.4 show the raw data of the number density of shish-like fibril crystals *N* vs. *t* for C-PE(230k)/L-PE(42k), C-PE(230k)/L-PE(104k), C-PE(130k)/L-PE(42k), and C-PE(86k)/L-PE(42k), respectively. It is obvious that *N* increases linearly against *t* and it is experimentally found saturation values of *N* (ν_{st}).

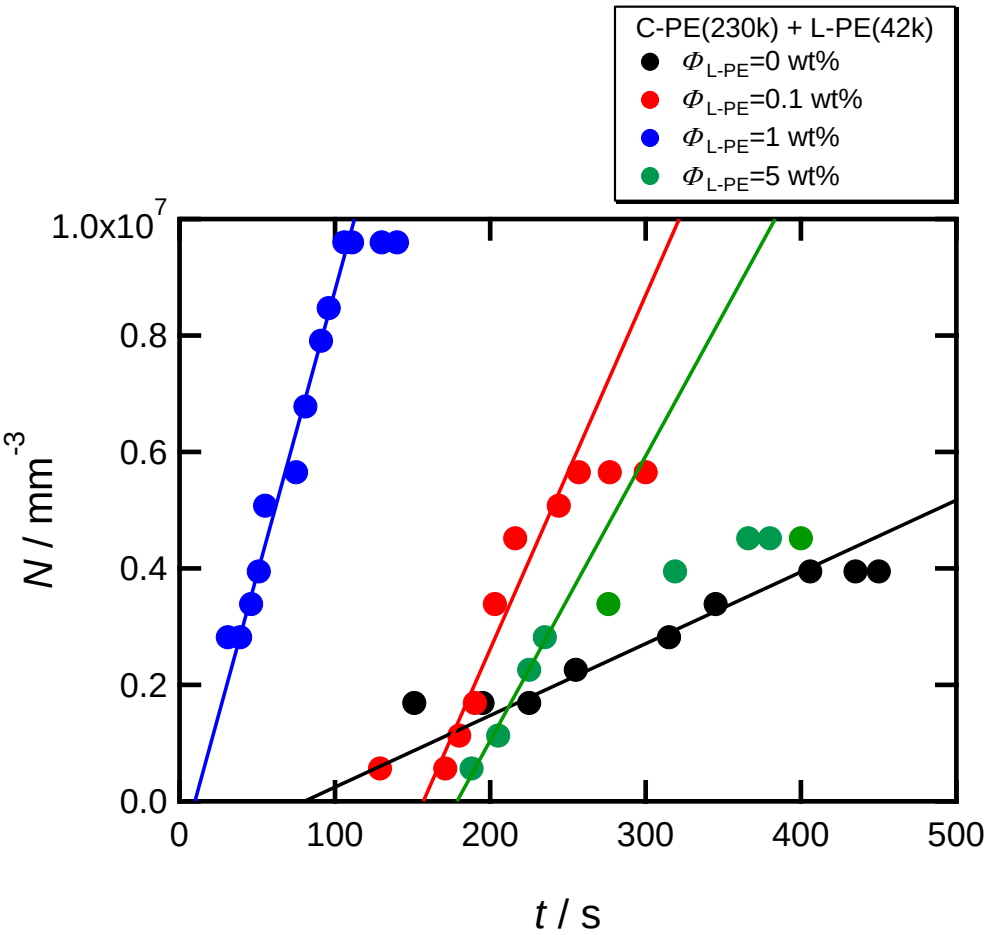

Figure S3.1 Plots of *N* vs. *t* for C-PE(230k)/L-PE(42k) blend system.

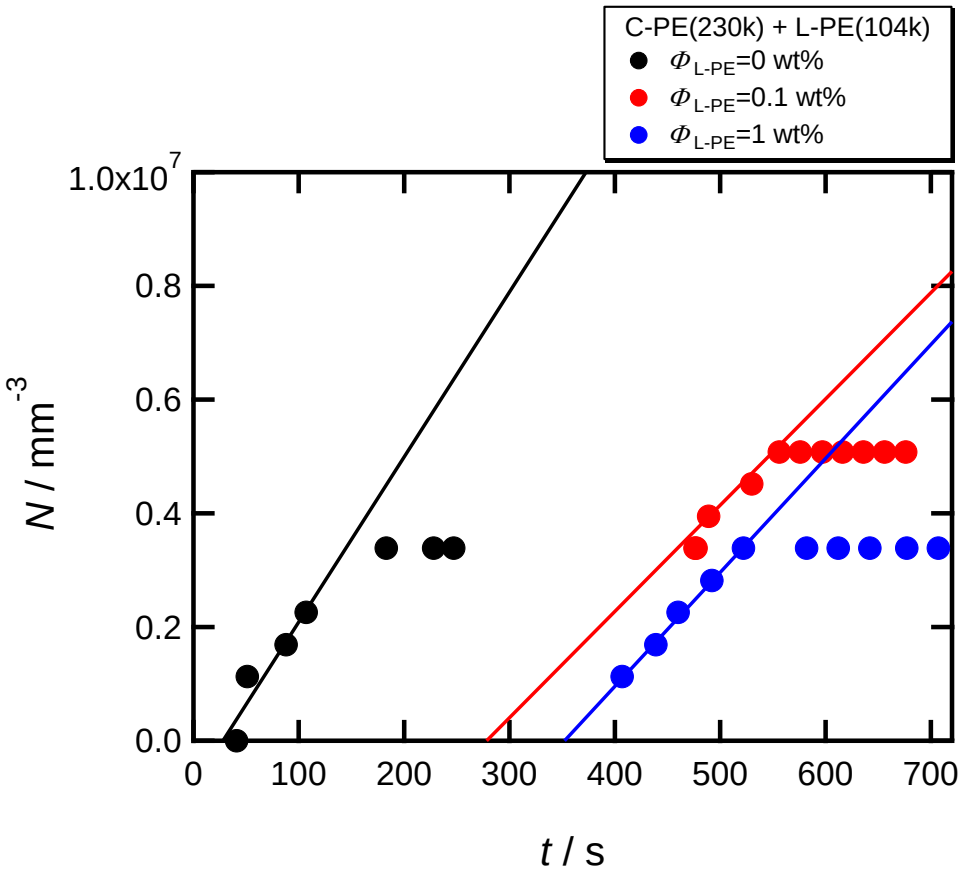

Figure S3.2 Plots of *N* vs. *t* for C-PE(230k)/L-PE(104k) blend system.

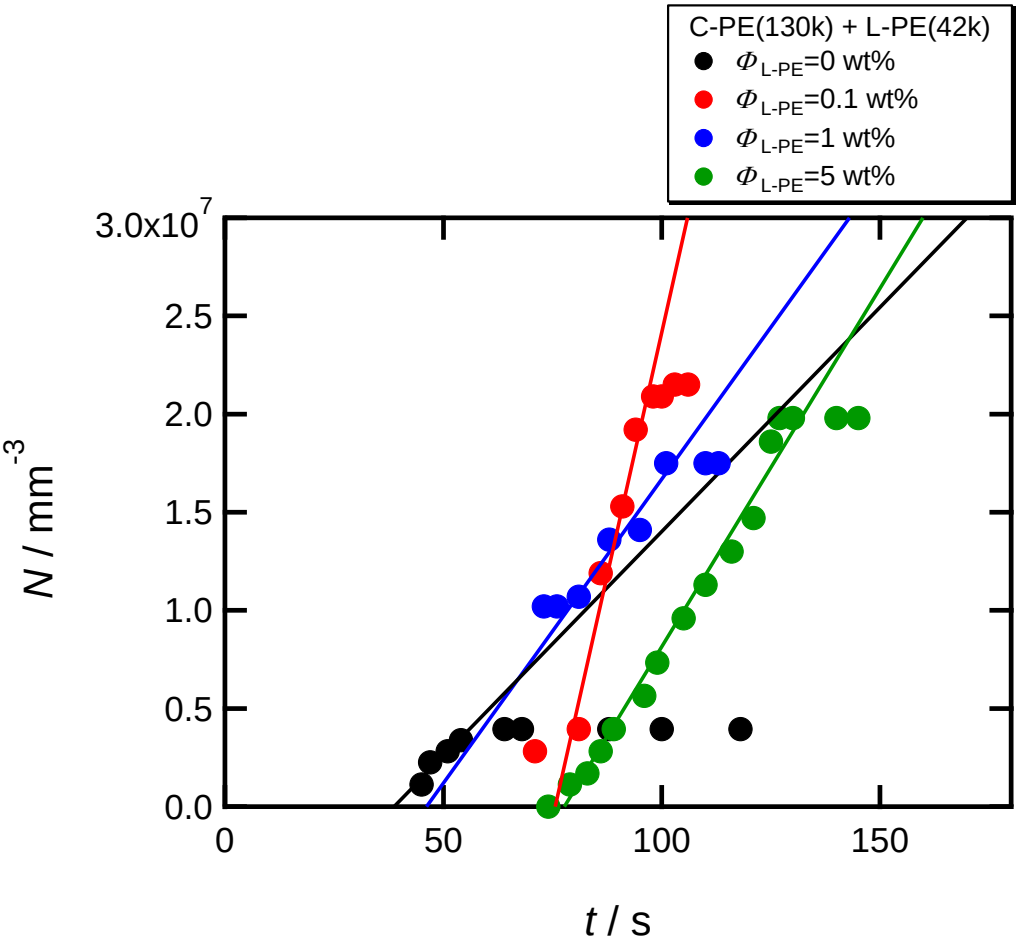

Figure S3.3 Plots of *N* vs. *t* for C-PE(130k)/L-PE(42k) blend system.

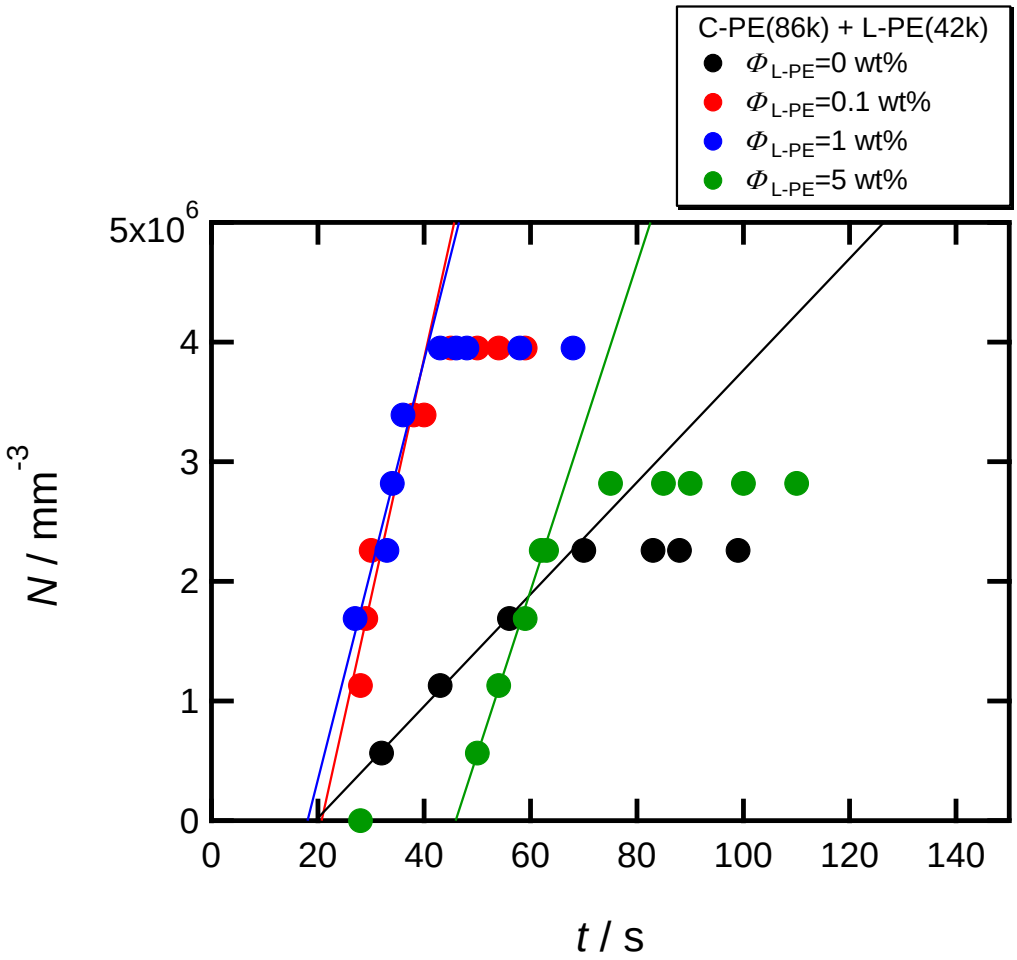

Figure S3.4 Plots of N vs. t for C-PE(86k)/L-PE(42k) blend system.

3-5-2 Variation of the saturation values of N (ν_{st}) against T_c and ε

To determine an appropriate T_c for a series of experiments, a broad survey of ν_{st} for a wide range of T_c was carried out in advance. **Figure S3.5** shows the plots of ν_{st} against T_c at constant strain (ε = 5) for the C-PE(230k)/L-PE(104k) blend system. It was found that ν_{st} of this sample is scattered in the range from ca. 1 to 5 mm^{-3}. A moderate crystallization temperature T_c = 120 °C was selected for this sample so that the shear condition can be changed widely in subsequent experiments. Because too low or high T_c needs to more mild or strong shear conditions for the formation of shish-like fibril crystals.

If such moderate T_c was not selected, there is almost no room to change the shear conditions.

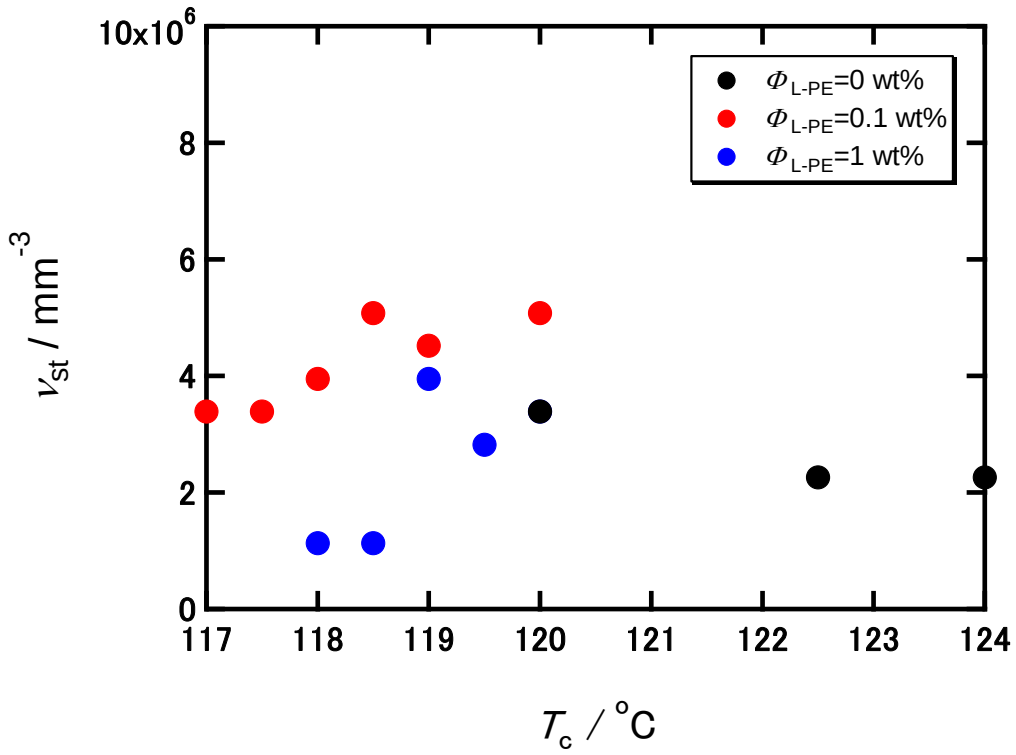

Figure S3.5 Plots of ν_{st} vs. T_c at a constant strain (ε = 5) for C-PE(230k)/L-PE(104k) blend system.

Figure S3.6 shows the plots of ν_{st} against ε at almost constant T_c (T_c = 119–120 °C) for all the samples used in this chapter. Even in the same shear strain, it was found that ν_{st} was significantly changed depending on $\Phi_{L\text{-}PE}$. Since too large or small ν_{st} will lead to unreliable I, the shear condition has to be selected carefully. Needless to say, if possible, applying consistent experimental conditions such as T_c and ε for all the samples with different $\Phi_{L\text{-}PE}$ should be desired.

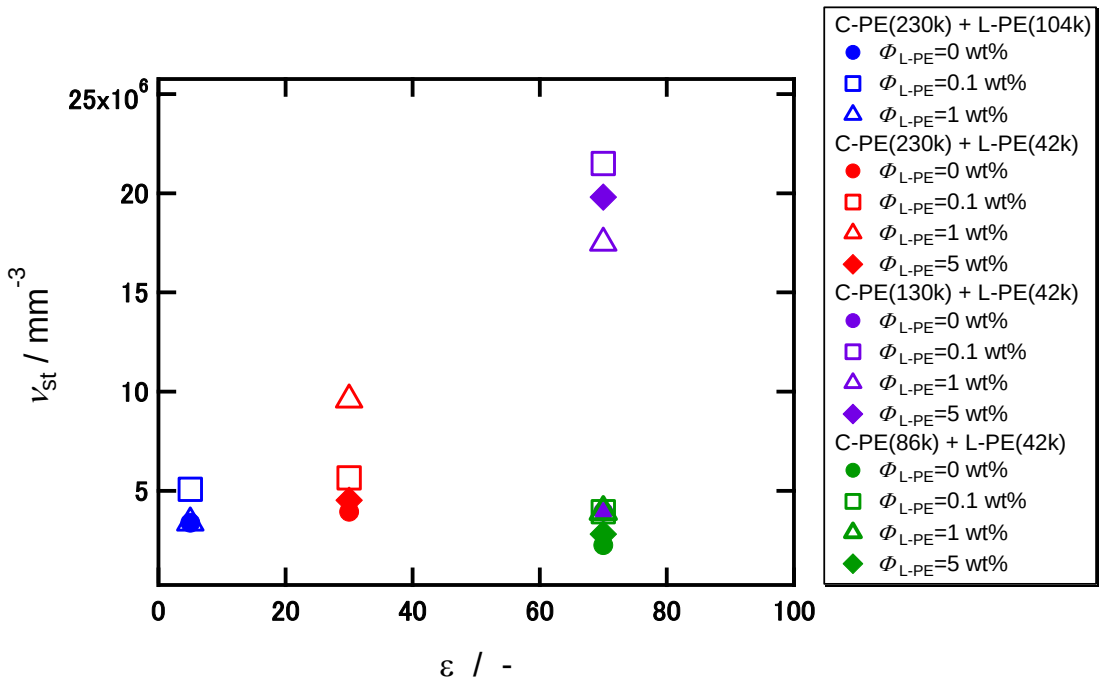

Figure S3.6 Plots of ν_{st} vs. ε for C-PE(230k)/L-PE(104k), C-PE(230k)/L-PE(42k), C-PE(130k)/L-PE(42k), and C-PE(86k)/L-PE(42k) blend systems.

3-6 References

[1] Keller A, Machin M J. Oriented crystallization in polymers. J Macromol Sci Part B: Phys. 1967;1:41–91.

[2] Keller A, Willmouth F M. Lattice orientation within stirring-induced crystals of polyethylene. J Macromol Sci Part B: Phys. 1972;B6:539–544.

[3] Pennings A J, Kiel A M, Fractionation of polymers by crystallization from solution, III. On the morphology of fibrillar polyethylene crystals grown in solution. Kolloid Z Z Polym. 1965;205:160–162.

[4] Pennings A J, van der Mark J M A A, Kiel A M. Hydrodynamically induced crystallization of polymers from solution. Colloid Polym Sci. 1970;237:336–358.

[5] Pennings A J. Bundle-like nucleation and longitudinal growth of fibrillar polymer crystals from flowing solutions. J Polym Sci: Polym Symp. 1977;59:55–86.

[6] Mitsuhashi S. On polyethylene crystals grown from flowing solutions in xylene. Bull Text Res Inst (J). 1963;66:1–9.

[7] Bashir Z, Odell J A, Keller A. High modulus filaments of polyethylene with lamellar structure by melt processing; the role of the high molecular weight component. J Mater Sci. 1984;19:3713–3725.

[8] Bashir Z, Odell J A, Keller A. Stiff and strong polyethylene with shish kebab morphology by continuous melt extrusion. J Mater Sci. 1986;21:3993–4002.

[9] Eder G, Janeschitz-Kriegl H, Liedauer S, Schausberger A, Stadlbauer W, Schindlauer G. The influence of molar mass distribution on the complex moduli of polymer melts. J Rheol. 1989;33:805–820.

[10] Liedauer S, Eder G, Janeschitz-Kriegl H, Jerschow P, Geymayer W, Ingolic E. On the kinetics of shear-induced crystallization in polypropylene. Int Polym Process. 1993;8:236–244.

[11] Liedauer S, Eder G, Janeschitz-Kriegl H. On the limitations of shear induced crystallization in polypropylene melts. Int Polym Process. 1995;10:243–250.

[12] Jerschow P, Janeschitz-Kriegl H. On the development of oblong particles as precursors for polymer crystallization from shear flow: Origin of the so-called fine grained layers. Rheol Acta. 1996;35:127–133.

[13] Jerschow P, Janeschitz-Kriegl H. The role of long molecules and nucleating agents in shear induced crystallization of isotactic polypropylenes. Int Polym Process. 1997;12:72–77.

[14] Keller A, Kolnaar H W H. Flow induced orientation and structure formation. In:

Meijer H (ed) Processing of polymers. Wiley-VCH, Weinheim. 1997;18:189–268.

[15] de Gennes P G. Coil-stretch transition of dilute flexible polymers under ultrahigh velocity gradients. J Chem Phys. 1974;60:5030–5042.

[16] Lieberwirth L, Loos J, Petermann J, Keller A. Observation of shish crystal growth into nondeformed melts. J Polym Sci Part B: Polym Phys. 2000;38:1183–1187.

[17] Somani R H, Yang L, Zhu L, Hsiao B S. Flow-induced shish-kebab precursor structures in entangled polymer melts. Polymer. 2005;46:8587–8623.

[18] Ogino Y, Fukushima H, Matsuba G, Takahashi N, Nishida K, Kanaya T. Effects of high molecular weight component on crystallization of polyethylene under shear flow. Polymer. 2006;47:5669–5677.

[19] Kumaraswamy G, Verma RK, Issaian A M, Wang P, Kornfield J A, Yeh F, Hsiao B S, Olley R H. Shear-enhanced crystallization in isotactic polypropylene Part 2. Analysis of the formation of the oriented “skin”. Polymer. 2000;41:8931–8940.

[20] Kumaraswamy G, Kornfield J A, Yeh F, Hsiao B S. Shear-enhanced crystallization in isotactic polypropylene. 3. Evidence for a kinetic pathway to nucleation. Macromolecules. 2002;35:1762–1769.

[21] Somani R H, Yang L, Hsiao B S. Precursors of primary nucleation induced by flow in isotactic polypropylene. Physica A. 2002;304:145–157.

[22] Sharma L, Ogino Y, Kanaya T. Shish kebab morphology induced in polyhydroxybutyrate under shear flow. Macromol Mater Eng. 2004;289:1059–1067.

[23] Yamazaki S, Watanabe K, Okada K, Yamada K, Tagashira K, Toda A, Hikosaka M. Formation mechanism of shish in the oriented melt (I)-bundle nucleus becomes to shish. Polymer. 2005;46:1675–1684.

[24] Yamazaki S, Watanabe K, Okada K, Yamada K, Tagashira K, Toda A, Hikosaka M.

Formation mechanism of shish in the oriented melt (II)-two different growth mechanisms along and perpendicular to the flow direction. Polymer. 2005;46:1685–1692.

[25] Dukovski I, Muthukumar M. Langevin dynamics simulations of early stage shish-kebab crystallization of polymers in extensional flow. J Chem Phys. 2003;118:6648–6655.

[26] Liang S, Wang K, Tang C, Zhang Q, Du R, Fu Q. Unexpected molecular weight dependence of shish-kebab structure in the oriented linear low density polyethylene/high density polyethylene blends. J Chem Phys. 2008;128:174902.

[27] Murase H, Kume T, Hashimoto T. Shear-induced structures in semidilute solution of ultrahigh molecular weight polyethylene at temperature close to equilibrium dissolution temperature. Macromolecules. 2005;38:6656–6665.

[28] Murase H, Kume T, Hashimoto T. Time evolution of structures under shear-induced phase separation and crystallization in semidilute solution of ultrahigh molecular weight polyethylene. Macromolecules. 2005;38:8719–8728.

[29] Murase H, Ohta Y, Hashimoto T. A new scenario of shish-kebab formation from homogeneous solutions of entangled polymers: Visualization of structure evolution along the fiber spinning line. Macromolecules. 2011;44:7335–7350.

[30] Murase H, Ohta Y, Hashimoto T. Shear-induced phase separation and crystallization in semidilute solution of ultrahigh molecular weight polyethylene: Phase diagram in the parameter space of temperature and shear rate. Polymer. 2009;50:4727–4736.

[31] Fukushima H, Ogino Y, Matsuba G, Nishida K, Kanaya T. Crystallization of polyethylene under shear flow as studied by time resolved depolarized light scattering. Effects of shear rate and shear strain. Polymer. 2005;46:1878–1885.

[32] Kanaya T, Matsuba G, Ogino Y, Nishida K. Hierarchic structure of shish-kebab by neutron scattering in a wide Q range. Macromolecules. 2007;40:3650–3654.

[33] Yang L, Somani R H, Sics I, Hsiao B S, Kolb R, Fruitwala H, Ong C. Shear-induced crystallization precursor studies in model polyethylene blends by in-situ rheo-SAXS and rheo-WAXD. Macromolecules. 2004;37:4845–4859.

[34] Kimata S, Sakurai T, Nozue Y, Kasahara T, Yamaguchi N, Karino T, Shibayama M, Kornfield J A. Molecular basis of the shish-kebab morphology in polymer crystallization. Science. 2007;316:1014–1017.

[35] Seki M, Thurman D W, Oberhauser J P, Kornfield J A. Shear-mediated crystallization of isotactic polypropylene: The role of long chain-long chain overlap. Macromolecules. 2002;35:2583–2594.

[36] Keum J K, Mao Y, Zuo F, Hsiao B S. Flow-induced crystallization precursor structure in high molecular weight isotactic polypropylene (HMW-iPP)/low molecular weight linear low density polyethylene (LMW-LLDPE) binary blends. Polymer. 2013;54:1425–1431.

[37] Roovers J. The melt properties of ring polystyrenes. Macromolecules. 1985;18:1359–1361.

[38] Roovers J. Viscoelastic properties of polybutadiene rings. Macromolecules. 1988;21:1517–1521.

[39] McKenna G B, Hostetter B J, Hadjichristidis N, Fetters L J, Plazek D J. A study of the linear viscoelastic properties of cyclic polystyrenes using creep and recovery measurements. Macromolecules. 1989;22:1834–1852.

[40] McKenna G B, Hadziioannou G, Lutz P, Hild G, Strazielle C, Straupe C, Rempp P, Kovacs A J. Dilute solution characterization of cyclic polystyrene molecules and their zero-shear viscosity in the melt. Macromolecules. 1987;20:498–512.

[41] Córdova M E, Lorenzo A T, Müller A J, Hoskins J N, Grayson S M. A comparative

study on the crystallization behavior of analogous linear and cyclic poly(ε-caprolactones). Macromolecules. 2011;44:1742–1746.

[42] Su H H, Chen H L, Díaz A, Casas M T, Puiggalí J, Hoskins J N, Grayson S M, Pérez R A, Müller A J. New insights on the crystallization and melting of cyclic PCL chains on the basis of a modified Thomson-Gibbs equation. Polymer. 2013;54:846–859.

[43] Shin E J, Jeong W, Brown H A, Koo B J, Hedrick J L, Waymouth R M. Crystallization of cyclic polymers: Synthesis and crystallization behavior of high molecular weight cyclic poly(ε-caprolactone)s. Macromolecules. 2011;44:2773–2779.

[44] Tezuka Y, Ohtsuka T, Adachi K, Komiya R, Ohno N, Okui N. A defect-free ring polymer: Size-controlled cyclic poly(tetrahydrofuran) consisting exclusively of the monomer unit. Macromol Rapid Commun. 2008;29:1237–1241.

[45] Takeshita H, Poovarodom M, Kiya T, Arai F, Takenaka K, Miya M, Shiomi T. Crystallization behavior and chain folding manner of cyclic, star and linear poly(tetrahydrofuran)s. Polymer. 2012;53:5375–5384.

[46] Ono R, Atarashi H, Yamazaki S, Kimura K. Molecular weight dependence of the growth rate of spherulite of cyclic poly(ε-caprolactone) polymerized by ring expansion reaction. Polymer. 2020;194:122403.

[47] Pérez R A, Córdova M E, López J V, Hoskins J N, Zhang B, Grayson S M, Müller A J. Nucleation, crystallization, self-nucleation and thermal fractionation of cyclic and linear poly(ε-caprolactone)s. React Funct Polym. 2014;80:71–82.

[48] Ferry J D. Viscoelastic properties of polymers. John Wiley & Sons, Inc.: New York; 1980.

[49] Kobayashi K, Saito Y, Yamazaki S, Kimura K. Role of entanglement species in the formation of shish-like fibril crystals elucidated by cyclic polyethylene. J Fiber Sci

Technol. accepted.

[50] Mills P J, Mayer J W, Kramer E J. Diffusion of polymer rings in linear polymer matrices. Macromolecules. 1987;20:513–518.

[51] Bielawski C W, Benitez D, Grubbs R H. An “Endless” route to cyclic polymers. Science. 2002;297:2041–2044.

[52] Fürstner A, Ackermann L, Gabor B, Goddard R, Lehmann C W, Mynott R, Stelzer F, Thiel O R. Comparative investigation of ruthenium-based metathesis catalysts bearing *N*-heterocyclic carbene (NHC) ligands. Chem Eur J. 2001;7:3236–3253.

[53] Bielawski, C W, Benitez D, Grubbs R H. Synthesis of cyclic polybutadiene via ring-opening metathesis polymerization: The importance of removing trace linear contaminants. J Am Chem Soc. 2003;125:8424–8425.

[54] Hahn S F. An improved method for the diimide hydrogenation of butadiene and isoprene containing polymers. J Polym Sci Part A: Polym Chem. 1992;30:397–407.

[55] Wunderlich B, Czornyj G. A study of equilibrium melting of polyethylene. Macromolecules. 1977;10:906–913.

[56] Broadhurst M G. Extrapolation of the orthorhombic *n*-paraffin melting properties to very long chain lengths. J Chem Phys. 1962;36:2578–2581.

[57] Broadhurst M G. The Melting Temperatures of the *n*-paraffins and the convergence temperature for polyethylene. J Res Natl Bur Stand A. 1966;70:481–486.

[58] Ogino Y, Fukushima H, Takahashi N, Matsuba G, Nishida K, Kanaya T. Crystallization of isotactic polypropylene under shear flow observed in a wide spatial scale. Macromolecules. 2006;39:7617–7625.

[59] Zhao Y, Hayasaka K, Matsuba G, Ito H. In situ observations of flow-induced precursors during shear flow. Macromolecules. 2103;46:172–178.

[60] Yamazaki S, Hikosaka M, Toda A, Wataoka I, Yamada K, Tagashira K. Nucleation and morphology of polyethylene under shear flow. J Macromol Sci Part B. 2003;42:499–514.

[61] Yamazaki S, Itoh M, Oka T, Kimura K. Formation and morphology of "shish-like" fibril crystals of aliphatic polyesters from the sheared melt. Eur Polym J. 2010;46:58–68.

[62] Pennings A J. Fractionation of polymers by crystallization from solutions. II. J Polym Sci Part C: Polym Sympo. 2007;16:1799–1812.

[63] Wang J, Bai J, Zhang Y, Fang H, Wang Z. Shear-induced enhancements of crystallization kinetics and morphological transformation for long chain branched polylactides with different branching degrees. Sci Rep. 2016;6:26560.

[64] Wunderlich B. Macromolecular physics. Vol 3. Crystal melting. Academic Press: New York; 1980.

[65] An Y, Holt J J, Mitchell G R, Vaughan A S. Influence of molecular composition on the development of microstructure from sheared polyethylene melts: Molecular and lamellar templating. Polymer. 2006;47:5643–5656.

[66] Pantani R, Coccorullo I, Volpe V, Titomanlio G. Shear-induced nucleation and growth in isotactic polypropylene. Macromolecules. 2010;43:9030–9038.

[67] Yang I-K, Wu C-H. Real-time SAXS measurements and rheological behavior of poly(lactic acid) crystallization under continuous shear flow. J Polym Res. 2014;21:609.

[68] Coccorullo I, Pantani R, Titomanlio G. Spherulitic nucleation and growth rates in an iPP under continuous shear flow. Macromolecules. 2008;41:9214–9223.

[69] Duplay C, Monasse B, Haudin J M, Costa J L. Shear-induced crystallization of polypropylene: Influence of molecular weight. J Mater Sci. 2000;35:6093–6103.

[70] Haas T W, Maxwell B. Effects of shear stress on the crystallization of linear

polyethylene and polybutene-1. Polym Eng Sci. 1969;9:225–241.

[71] Wolkowicz M D. Nucleation and crystal growth in sheared poly(1-butene) melts. J Polym Sci: Polym Symp. 2007;63:365–382.

[72] Huo H, Meng Y, Li H, Jiang S, An L. Influence of shear on polypropylene crystallization kinetics. Eur Phys J E. 2004;15:167–175.

[73] Lagasse R R, Maxwell B. An experimental study of the kinetics of polymer crystallization during shear flow. Polym Eng Sci. 1976;16:189–199.

Concluding Remarks

This thesis revealed the role of entanglements of polymer crystallization under the quiescent and flow field. The role of entanglements in polymer crystallization is one of the most important irrespective of the quiescent and flow field and has not been clarified well. Cyclic polymers have a unique feature in that entanglement species are restricted compared with linear polymers. The entanglements formed between cyclic and linear polymers are especially of interest.

In Chapter 1, to clarify the role of novel entanglements formed between cyclic and linear polymers during crystallization, the isothermal crystallization behavior of blends of cyclic polyethylene (C-PE) and linear polyethylene (L-PE) in a quiescent state was investigated. The samples were prepared by mixing the prepared C-PE and L-PE at the weight fraction of L-PE ($\Phi_{\text{L-PE}}$) of 0–100 wt%, with the weight average molecular weight (M_w) of C-PE and L-PE being 175×10^3 and 154×10^3, respectively. The isothermal crystallization behavior was analyzed through polarizing optical microscopy (POM) and differential scanning calorimetry (DSC). The morphology observed by POM was similar to that of $\Phi_{\text{L-PE}}$. From the time evolution of the heat flow measured via DSC, the half-crystallization time ($t_{1/2}$) was obtained as a function of $\Phi_{\text{L-PE}}$ at different degrees of supercooling (ΔT). The $1/t_{1/2}$ values of the C-PE and L-PEhomopolymers were almost the same at ΔT = 27 K. At a lower ΔT, the $1/t_{1/2}$ values of the C-PE was significantly larger than that of L-PE, and vice versa at a larger ΔT. In contrast, the $1/t_{1/2}$ value reached a minimum at $\Phi_{\text{L-PE}}$ = 50 wt%, irrespective of ΔT. As the entanglement density increased with increasing $\Phi_{\text{L-PE}}$, the crystallization rate was expected to decrease monotonically. Considering the experimental relationship between $1/t_{1/2}$ and $\Phi_{\text{L-PE}}$, it was speculated that

the suppression of crystallization in the blended system is caused by a novel entanglement formed by the penetration of the L-PE chain into the C-PE chain.

In Chapter 2, to clarify the role of entanglement species in the formation of shish-like fibril crystals, the shear-induced crystallization behaviors of C-PE, L-PE, and C-PE and L-PE blends were investigated using a hot stage equipped with a polarizing optical microscope. The shear-induced crystallization behavior of the C-PE(115k) and L-PE(65k) homopolymers, where the values in parentheses represent the molecular weights (M_w), indicated that the formation rate of the shish-like fibril crystals of the former was one order of magnitude smaller than that of the latter. This implies that it is more difficult for C-PE to form shish-like fibril crystals than L-PE due to the topological effect of C-PE; that is, C-PE chains are more difficult to elongate by shear than L-PE chains due to the lack of chain ends. The shear-induced crystallization behavior of the blended C-PE and L-PE samples provided further insight into the effect of entanglement species on the formation of shish-like fibril crystals. The addition of small amounts of L-PE to C-PE remarkably enhanced the formation rate and density of the shish-like fibril crystals. The influence of the novel entanglement formed by the penetration of the L-PE molecule into the C-PE ring on the formation of the oriented melt was speculated to be significant.

In Chapter 3, the shear-induced crystallization behavior of a blend of C-PE and L-PE. Using C-PE as a matrix and L-PE as an additive was investigated. The molecular weight and blend ratio of C-PE and L-PE were changed and the formation rate of shish-like fibril crystals (I) was measured. In both blend systems of C-PE(230k)/L-PE(42k) and C-PE(230k)/L-PE(104k), where the values in parentheses represent the molecular weight, I reached a maximum at a certain weight fraction of L-PE, $\Phi_{\text{L-PE}}$. As the $\Phi_{\text{L-PE}}$ was increased, that is, the entanglement density was increased, the formation of the oriented

melt was promoted while crystallization was simultaneously suppressed by entanglements. The maximum value of *I* was observed owing to these two competing factors. Similar behavior was observed in the blend systems of C-PE(230k)/L-PE(42k), C-PE(130k)/L-PE(42k), and C-PE(86k)/L-PE(42k). These results imply that the formation of shish-like fibril crystals in the blended samples of C-PE and L-PE was determined by these competing effects.

List of publications

1. Formation of shish-like fibril crystals from the melt of blends of cyclic and linear polyethylene under shear flow

   Keiko Kobayashi, Shinichi Yamazaki, Kunio Kimura

   Polymer Journal, Vol 54, No. 7, pp. 913–920 (2022)

2. Role of entanglement species in the formation of shish-like fibril crystals elucidated by cyclic polyethylene

   Keiko Kobayashi, Yuya Saito, Shinichi Yamazaki, Kunio Kimura

   Journal of Fiber Science and Technology, accepted.

3. Effect of blend ratio of cyclic and linear polyethylene blends on isothermal crystallization in quiescent state

   Keiko Kobayashi, Hironori Atarashi, Shinichi Yamazaki, Kunio Kimura

   to be submitted to *Polymer Journal*.

Acknowledgments

I would like to express my deepest and heartfelt gratitude to Professor Dr. Kunio Kimura, Graduate School of Environmental and Life Science, Okayama University, for his special guidance, numerous helpful suggestions, cordial direction and continuous encouragement throughout this experimental research work.

I would like to express my deepest and heartfelt gratitude to Associate Professor Dr. Shinichi Yamazaki, Graduate School of Environmental and Life Science, Okayama University, for his proper guidance, untiring efforts, valuable advice, numerous fruitful discussion, constant and warm encouragement and throughout this work. I greatly appreciate that he gave me many precious chances to present this research work at not only the internal but also the international conferences.

I am greatly and deeply indebted to Assistant Professor Dr. Hironori Atarashi, Graduate School of Environmental and Life Science, Okayama University, for his special guidance, numerous helpful suggestions, cordial direction and continuous encouragement throughout this experimental research work.

I am greatly and deeply indebted to Professor Dr. Yukitaka Kimura, Graduate School of Environmental and Life Science, Okayama University, for his special guidance, numerous helpful suggestions, cordial direction and continuous encouragement.

I am greatly and deeply indebted to Senior Assistant Professor Dr. Tomoyuki Tajima, Graduate School of Environmental and Life Science, Okayama University, for his special guidance, numerous helpful suggestions, cordial direction and continuous encouragement.

I wish to thank Research Professor Dr. Tetsuya Uchida, Graduate School of Natural Science and Technology, Okayama University, for his helpful suggestion and sound advice.

I wish to thank Senior Assistant Professor Dr. Takumi Okihara, Graduate School of Natural Science and Technology, Okayama University, for his helpful suggestion and sound advice.

I conclude my acknowledgement by extending my science thanks to all members, past and present of Kimura laboratory for their cooperation and friendship throughout my study here.

The Author

Keiko Kobayashi

Keiko Kobayashi

Graduate School of Environmental and Life Science,

Okayama University

3-1-1, Tsushima-naka, kita-ku, Okayama 700-8530

JAPAN

March 2023